



Improved operational stability of Pebax-based gas separation membranes with ZIF-8: A comparative study of flat sheet and composite hollow fibre membranes



Putu Doddy Sutrisna^a, Jingwei Hou^{a,*}, Hongyu Li^a, Yatao Zhang^{a,b}, Vicki Chen^a

^a UNESCO Centre for Membrane Science and Technology, School of Chemical Engineering, University of New South Wales, Sydney, NSW 2052, Australia

^b School of Chemical Engineering and Energy, Zhengzhou University, Zhengzhou 450001, PR China

ARTICLE INFO

Keywords:

ZIF-8
Pebax-1657
Plasticization
Compaction
Gas separation

ABSTRACT

Polymer-based hollow fibre composite membranes are composed of a porous support coated with a highly permeable gutter layer, and a thin selective top layer. They are promising candidates for industrial gas separation, but there are challenges in maintaining their performance under high pressure or during long-term operation. To tackle this, we incorporated ZIF-8 into Pebax-1657 (polyamide-polyether copolymer) for gas separation membrane fabrication. To fully understand the behaviour of hollow fibre composite membranes, special attention was paid to the effect of ZIF-8 on the Pebax chain structure using dense film flat sheet membranes. The presence of porous ZIF-8 disrupted the original well-packed polymer chain structure, leading to higher fractional free volume and gas permeability. However, the introduced microvoids were non-continuous and the gas selectivity was only slightly reduced. On the other hand, the stable structure of ZIF-8, together with the hydrogen bonds between ZIF-8 organic ligands and polyamide chains, significantly improved the linear glassy polymer chain stiffness, ensuring good operational stability under elevated pressure for both flat sheet and hollow fibre membranes. Finally, good long-term operational stability was observed with the hollow fibre membrane, indicating the ZIF-8/Pebax coating overcame the aging previously observed for the poly[1-(trimethylsilyl)-1-propyne] (PTMSP) gutter layer.

1. Introduction

Gas separation has been considered as an important part of energy and environmental sciences. Pressure swing adsorption and cryogenic distillation are the most common approaches for large-scale gas separation. However, their high energy demand and large physical footprint are the main drawbacks of these conventional separation techniques [1,2]. Some other novel techniques like biocatalytic gas separation process are still at their infancy stage thus haven't been tested for large-scale application [3]. In comparison, membrane-based gas separation permits easier operation, lower energy consumption and smaller footprint. Thus it has received increasing research attention for flue gas separation, natural gas sweetening and hydrogen purification [4–6]. The polymeric membrane is currently considered the most promising candidate for industrial application in gas separation due to their lower price and easier processing. The gas transport through the polymeric membrane follows the solution-diffusion mechanism, and the overall efficiency is determined by the diffusivity and solubility of certain gas molecules within the membrane matrix [7,8].

Both glassy and rubbery polymers have been applied to fabricate gas separation membranes. For the rubbery polymers with flexible chains, the gas-selective transport is achieved by the favorable interactions between gas molecules and polymer chains. While for the glassy polymers, the size discrimination also plays an important role in gas separation [9–11]. However, there exists a gas permeability-selectivity trade-off upper bound, which was compiled by Robeson in 1991 by plotting the logarithmic of gas permeability and selectivity of different gas pairs for the performance of existing gas separation membranes [12]. The upper bound has been updated with the rapid development of new membrane materials in recent years [13,14].

One effective way to improve the polymeric membrane performance beyond the upper bound is to incorporate inorganic nanofillers within the membrane matrix [8,9,15]. Recently, metal organic frameworks (MOFs), especially zeolitic imidazolate frameworks (ZIFs), has received a growing interest as potential fillers in the mixed matrix membranes. There have been several successful demonstrations of improving the membrane permeability by mixing ZIFs and polymer materials [16–19]. On the other hand, the capability of gas separation membranes to

* Corresponding author.

E-mail address: Jingwei.hou@unsw.edu.au (J. Hou).

handle high-pressure feed gases is considered as the pre-requisition of their practical application in natural gas sweetening and hydrogen purification, as it eliminates the needs of feed depressurization and permeate re-pressurization. However, the exposure of the polymeric membrane to high-pressure conditions can lead to swelling of the polymer chains (glassy polymer) or irreversible compaction/crystallization (rubbery polymer) [20,21]. It has been demonstrated that the incorporation of ZIFs can mitigate these detrimental effects for the mixed matrix dense membranes, as the presence of ZIFs rigidifies the surrounding polymer chains especially for the glassy polymers (e.g. polyimide) [16,17,22].

Although the improved performance has been observed with the mixed matrix dense membranes, thin composite hollow fibre membranes are more competitive for large-scale industrial application due to their higher gas permeation rate and lower consumption of expensive materials during the fabrication process. The composite membrane usually consists of a highly permeable gutter layer and a surface ultrathin selective layer, both of which are coated on a porous membrane support. Poly(dimethylsiloxane) (PDMS) and poly[1-(trimethylsilyl)-1-propyne] (PTMSP) are the most commonly applied gutter layer to bridge the porous support and thin selective layer. But the formation of a thin, defect-free selective coating layer on PDMS can be challenging due to its low surface energy, leading to poor interfacial adhesion between the gutter layer and the selective layer [15,23]. To tackle this problem, researchers have developed a series of flat sheet composite membranes using surface-functionalized PDMS to introduce the addition of a thin selective layer, and the incorporation of inorganic nanoparticles, star-polymers and soft nanoparticles can promote the composite membrane gas permeability [24–28]. Similarly, Li et al. [29] applied polydopamine as an intermediate layer between PDMS and polyvinylamine (PVAm) selective layer. On the other hand, the application of PTMSP, one of the most permeable polymer material, as the gutter layer has been limited because the gradual relaxation of its porous structure can lead to a significant loss of permeance especially for thin films [30–32]. For example, the dip-coated bare PTMSP thin layer can lose nearly 80% of its original permeance after 10 days at room temperature [4]. However, for the composite membrane whether the coating of a selective polymer layer can stabilize the non-equilibrium PTMSP structure has not been fully explored. In addition, as discussed above, the membrane stability under an elevated pressure condition is crucial for the practical application. However, this aspect is still relatively poorly understood for composite membranes. As the thin polymer layer has inferior structural stability, the pressure-induced deformation or plasticization can be more significant [33]. Fu et al. [25] studied the performance of the flat sheet composite membrane with a feed pressure up to 10 bar of pure CO₂, and the slight plasticization was observed of the thin selective layer. But whether the self-supporting hollow fibre composite membrane can sustain high feed pressure is of significant practical importance and thus worth investigating.

These critical issues were addressed in this work. ZIF-8 and Pebax-1657, a commercial block copolymer containing linear glassy poly-

amide and rubbery poly(ethylene oxide), were applied to fabricate both mixed matrix dense flat sheet membranes and hollow fibre composite membranes. Both PDMS and PTMSP were investigated as the composite membrane gutter layers. The effect of ZIF-8 on the membrane performance was systemically investigated, and special attention was paid to bridge the flat sheet characterization results and the composite hollow fibre membrane performance. In addition, the performance of both flat sheet and hollow fibre membranes under an elevated pressure condition was studied using CO₂ and CH₄ as feed gases. Complete pressurization-depressurization cycles were applied to understand the reversibility of the high-pressure induced polymer structure change. Finally, the long-term stability of the hollow fibre composite membrane was explored to test the effect of the thin selective layer on the aging behaviour of the PTMSP gutter layer.

2. Materials and methods

2.1. Materials

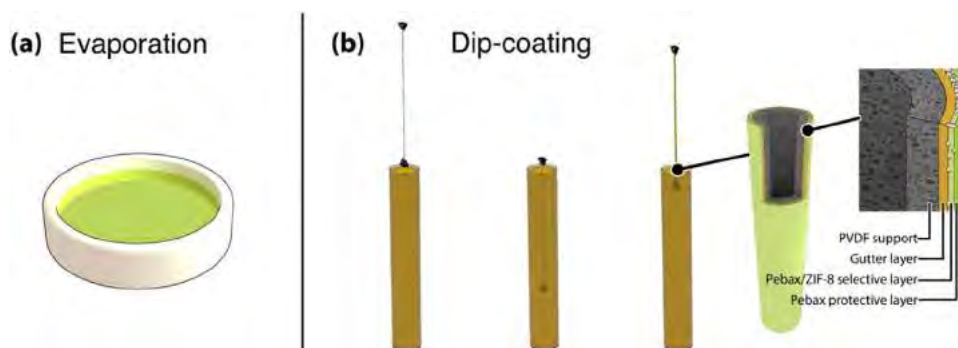
Polyether oxide - polyamide (PEO-PA) blocks (Pebax[®] 1657) polymer supplied by Arkema was used as the polymer matrix for both flat sheet and hollow fibre membranes. Pebax-1657 applied in this work contained 60% rubbery phase and 40% glassy phase. Zinc nitrate hexahydrate and 2-methylimidazole supplied by Sigma-Aldrich were used for ZIF-8 preparation and methanol was used as the solvent. Poly[1-(trimethylsilyl)-1-propyne] (PTMSP) and poly(dimethylsiloxane) (PDMS) used as the gutter layer for hollow fibre composite membranes were kindly supplied by Gelest, Inc., PA, USA and Dow Corning, Australia. Polyvinylidene fluoride (PVDF) hollow fibres porous support was kindly provided by Beijing Origin Water Technology Co., Ltd. (China) with a diameter around 1 mm and a pore size of 0.05 μm. Both pure and mixed gases for the permeation test were purchased from Coregas. All other chemicals were of the highest purity and used without further purification.

2.2. Synthesis of ZIF-8 nanoparticles

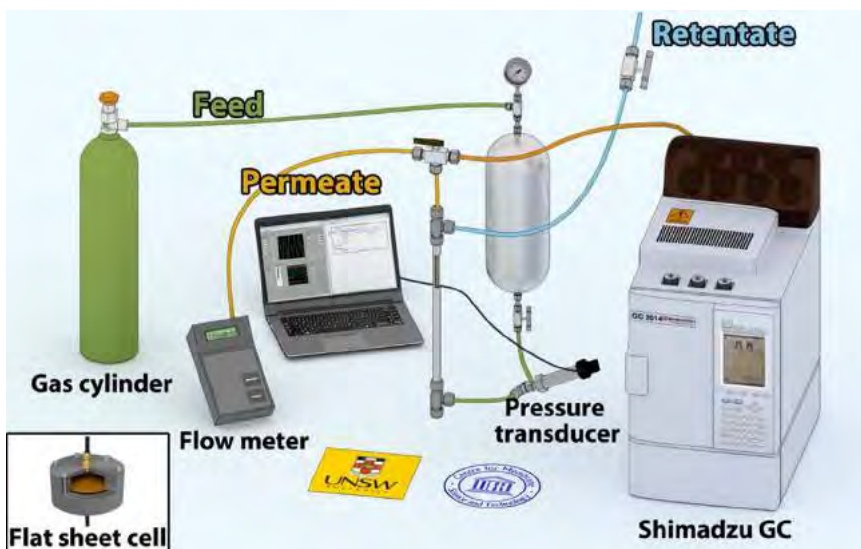
ZIF-8 was prepared in-house in this work following the steps reported elsewhere [34]. Briefly, 6.5 g of 2-methylimidazole was dissolved in 200 ml methanol and then mixed with a 200 ml methanol solution containing 3 g of zinc nitrate hexahydrate. The mixture was vigorously stirred for one hour and until it gradually turned cloudy. The suspension solution was then separated using a Beckman Avanti centrifuge for 15 min at 13,000 rpm, followed by another two cycles of re-suspension and centrifugation cycles with pure methanol to remove the unreacted chemicals.

2.3. Fabrication of the Pebax-based flat sheet mixed matrix membranes

The solvent evaporation technique was applied for membrane



Scheme 1. Fabrication of the (a) flat sheet and (b) hollow fibre composite membranes.



Scheme 2. Experimental rig for the gas permeation test.

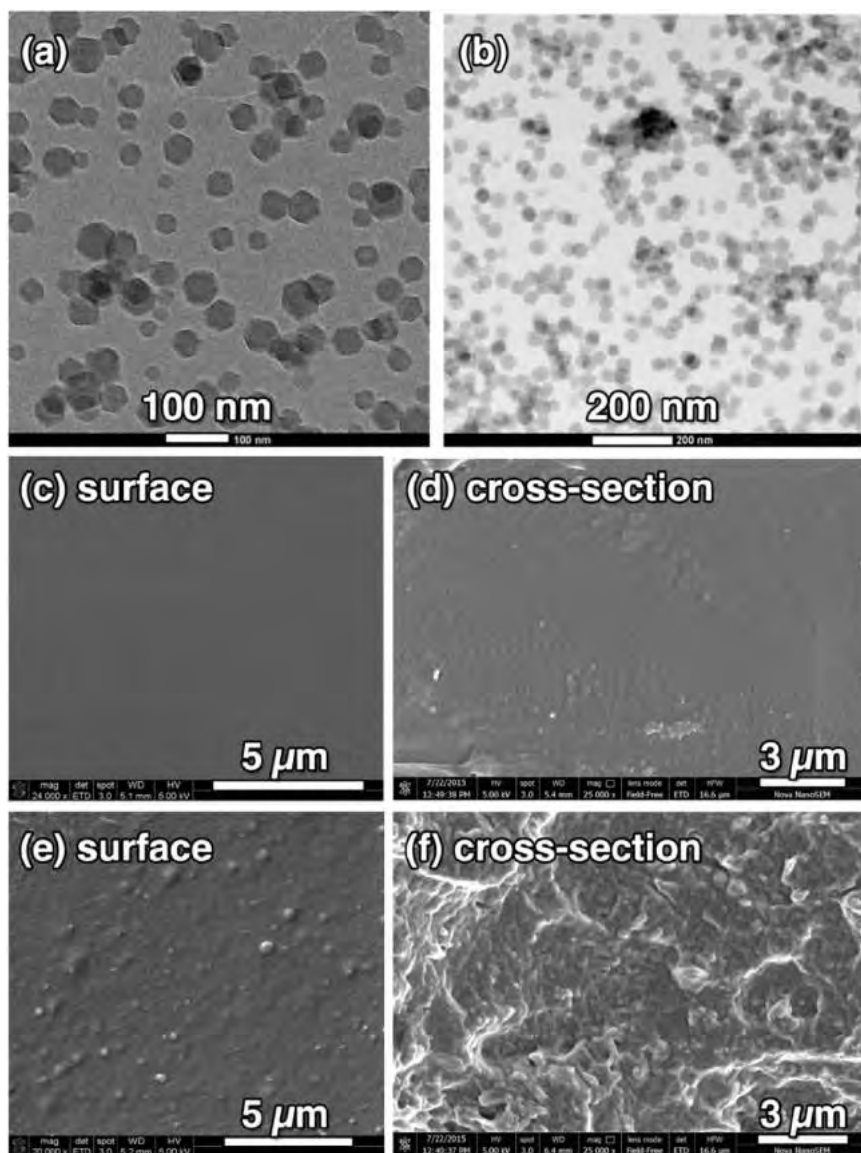


Fig. 1. (a-b) TEM image of the in-house prepared ZIF-8 nanoparticles. SEM images of (c-d) pure Pebax membrane and (e-f) mixed matrix membrane containing 20 wt% ZIF-8.

Table 1Glass transition temperature (T_g) and degree of crystallinity of Pebax based mixed matrix membranes (showing the T_g of PEO only; typical error of T_g was ~ 0.5 °C).

Sample name	Integral of melting point (J/g)		T_g (°C)	X_{PEO} (%)	X_{PA} (%)	X_c (total) (%) ^a	X_c (total) (%) ^b
	PEO block	PA block					
Pure Pebax	13.77	21.2	-58.2	13.79	23.04	17.49	16.3
MMM 3 wt% ZIF-8	16.19	21.45	-58.0	16.21	23.31	19.05	19.38
MMM 10 wt% ZIF-8	17.05	21.5	-56.0	17.08	23.37	19.59	19.76
MMM 20 wt% ZIF-8	20.75	23.61	-55.5	20.78	25.66	22.73	22.48

^a Degree crystallinity of membrane from DSC analysis.^b Degree crystallinity of membrane from XRD analysis.**Table 2**

Density, specific volume and FFV of Pebax-based membranes.

Sample	Density, ρ (g/cm ³)	FFV	BET surface area (m ² g ⁻¹)
ZIF-8 [40]	0.95	0.475	1,639
Pure Pebax-1657	1.130 \pm 0.019	0.154 \pm 0.002	Not detected
3 wt% ZIF-8/Pebax	1.097 \pm 0.023	0.167 \pm 0.002	0.0153
10 wt% ZIF-8/Pebax	1.053 \pm 0.022	0.192 \pm 0.008	0.0401
20 wt% ZIF-8/Pebax	0.963 \pm 0.025	0.226 \pm 0.009	0.0566

preparation (Scheme 1a). The Pebax-1657 polymer was dissolved in water/ethanol solution (30/70, w/w, 70 °C) with a concentration of 3 wt% under constant stirring and reflux. Then ZIF-8 nanoparticles were added into the polymer solution at room temperature. ZIF-8 concentration was 3, 10 or 20 wt% with the respect to the polymer dry weight. The loading of ZIF-8 corresponded to 3.7, 12.3 and 24.6 vol% calculated based on the density. The priming protocol was adopted to ensure a good dispersion of ZIF-8 within the polymer. After degassing overnight, 25 ml of casting solution was poured into a Teflon dish (13 cm in diameter) and left at room temperature until it started to peel off. The prepared membrane was annealed under vacuum at 50 °C for 3 days before tested in a gas permeation rig.

2.4. Fabrication of ZIF-8/Pebax-1657 based hollow fibre membrane

The composite membrane fabrication process is presented in Scheme 1b. Specifically, the gutter layer coating solutions were 2 wt% PTMSP (n-hexane as solvent) or 3 wt% PDMS (n-hexane as solvent), and the selective layer coating solution contained 3 wt% Pebax and 0–30 wt% of ZIF-8 (with the respect to the polymer dry weight). In terms of the coating, PVDF membranes were pre-soaked in Milli-Q water for 24 h and then the outer surface was briefly dried using Kimwipe tissues. This was to minimize the penetration of the gutter layer into PVDF membrane pores. The dip-coating parameters were: 1 cm/s lowering speed, 1 min soaking time and 0.4 cm/s withdrawn speed. Both ends of the hollow fibre were sealed to only coat the outer surface. The coating cycles were 4 cycles for the gutter layer, 2 cycles for the selective layer, and 1 cycle for the protective layer (pure Pebax). Between each coating cycle, the membrane was dried for 8 h inside an oven at 50 °C.

2.5. ZIF-8 particles and membranes characterization

ZIF-8 nanoparticles were analysed using FEI Tecnai G2 20 TEM for imaging purpose. The specific surface area and the pore volume of ZIF-8 nanoparticles were analysed using nitrogen adsorption-desorption isotherms at 77 K in a Micromeritic Tristar 3000 analyzer. The particle size distribution was examined by the Malvern Nano dynamic light scattering, by dispersing the particles in ethanol and sonicating for 1 min.

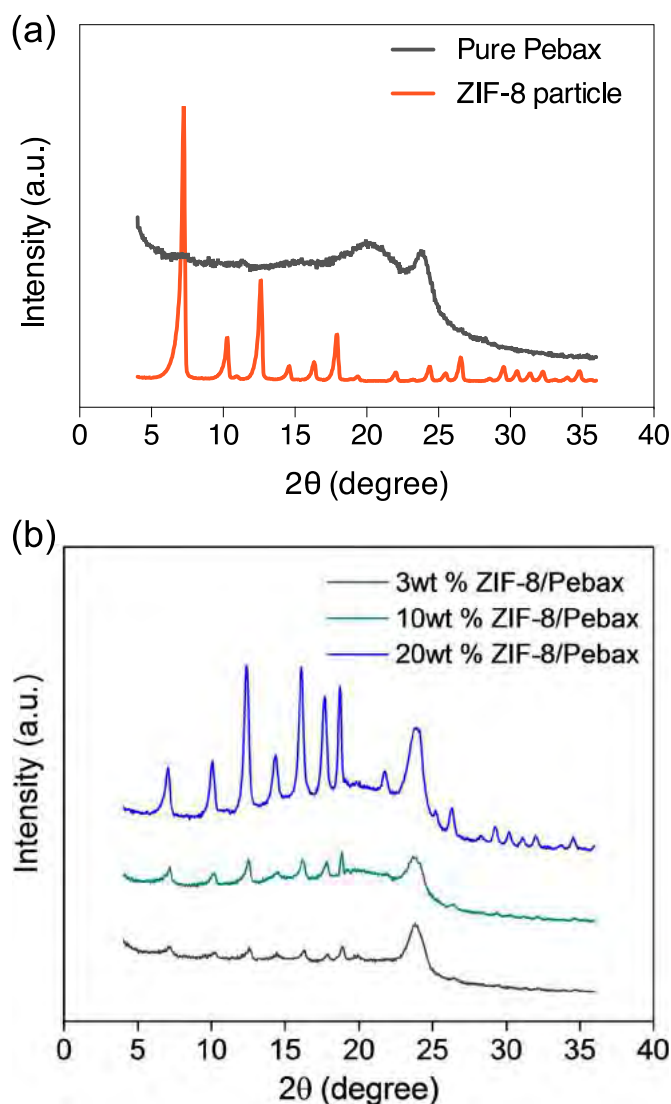


Fig. 2. XRD patterns of (a) pure Pebax membrane and ZIF-8 particle; (b) ZIF-8/Pebax mixed matrix membranes.

For the membrane samples, the surface and cross-sectional images were examined in FEI Nova NanoSEM 230 FESEM after the membrane sample was coated with a layer of chromium. The presence of ZIF-8 and the quality of dispersion in the membrane matrix were examined with EDX (FEI Nova NanoSEM 230 FESEM). The samples were coated with a layer of carbon prior to the EDX test. The determination of glass transition temperature of membranes was conducted with DSC analysis (Mettler Toledo DSC 823e analyzer) from 100 °C to 250 °C for two cycles. The crystallinity of ZIF-8 and the membranes were analysed in a PANalytical Empyrean Thin-Film XRD device for 2θ from 4° to 36°

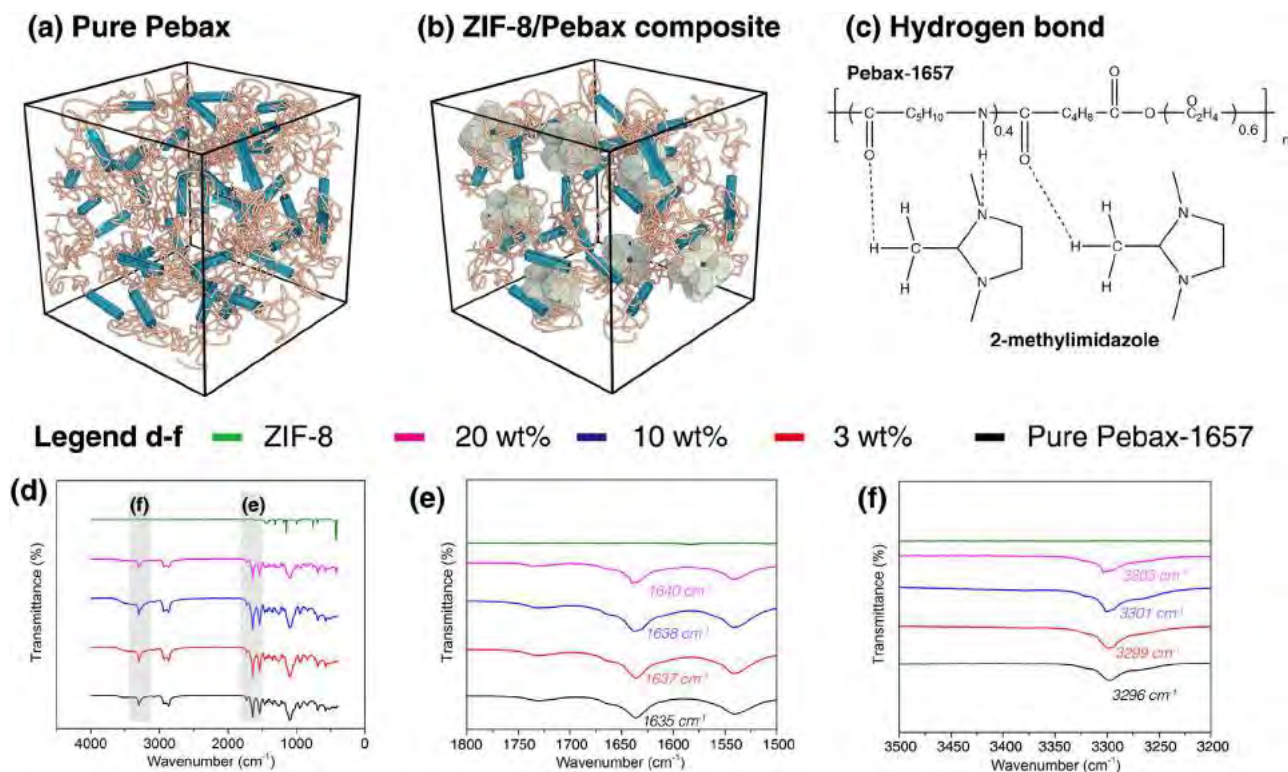


Fig. 3. Effect of ZIF-8 on the Pebax polymer structure. Polymer chain structures for (a) pure Pebax and (b) Pebax/ZIF-8 composite, (c) formation of hydrogen bonds between ZIF-8 and PA, and (d–f) FT-IR spectra of ZIF-8, pure Pebax and the mixed matrix membranes.

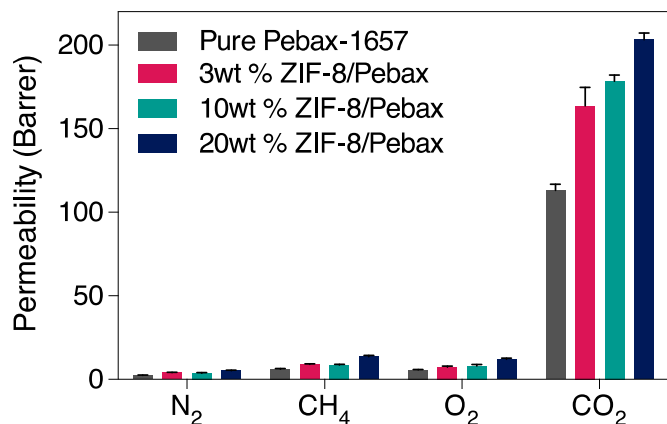


Fig. 4. Pure gas permeability of the pure Pebax and the mixed matrix membranes with 3, 10 and 20 wt% of ZIF-8 (feed pressure 3 bar and 25 °C).

Table 3

Ideal gas selectivity of the pure Pebax and the mixed matrix membranes (feed pressure 3 bar and 25 °C).

	Pure Pebax membrane	3 wt% ZIF-8 in Pebax membrane	10 wt% ZIF-8 in Pebax membrane	20 wt% ZIF-8 in Pebax membrane
$\alpha_{\text{CO}_2/\text{N}_2}$	47.0 ± 0.5	41.9 ± 1.6	41.2 ± 0.6	41.1 ± 1.6
$\alpha_{\text{CO}_2/\text{CH}_4}$	19.4 ± 0.1	19.1 ± 0.3	19.2 ± 0.4	15.1 ± 0.2
$\alpha_{\text{CO}_2/\text{O}_2}$	19.7 ± 0.1	23.4 ± 0.35	19.5 ± 0.5	17.13 ± 0.6
$\alpha_{\text{O}_2/\text{N}_2}$	2.4 ± 0.04	1.8 ± 0.1	2.1 ± 0.1	2.4 ± 0.05

with 0.026° step size. The interactions between ZIF-8 nanoparticles and Pebax polymer chains within the mixed matrix membranes were examined by the Fourier transform infrared analyzer with wave number in the range of 400–4000 cm⁻¹ (FTIR, Bruker Alpha).

The density of flat sheet membrane was estimated by measuring the

weight of a 2.5×2.5 cm² sample with a microbalance and the volume of the sample was estimated with the measured thickness (average of five measurements at different locations on the sample). The density data were used to calculate the fractional free volume (FFV) of the polymer. FFV is a semi-empirical parameter that represents molecular scale space or opening of adequate size close to gas molecules to accommodate gas molecules thus allow a diffusion step. These molecular spaces are the sum of many small spaces between polymer chains [35,36] and usually defined as

$$FFV = \frac{V - V_o}{V} \quad (1)$$

where V is the specific volume of the polymer, V_o is the volume occupied by the molecules that can be estimated using Bondi group contribution method: the occupied volume is calculated from the van der Waals volumes, V_{LW} , of the various groups in the polymer structure [37]:

$$V_o = 1.3 V_w \quad (2)$$

The FFV of mixed matrix membrane can be calculated using Eq. (3) [38]:

$$FFV_{MMM} = FFV_{polymer} \cdot \phi_{polymer} + FFV_{filler} \cdot \phi_{filler} \quad (3)$$

where ϕ is fractional volume and FFV_{filler} is derived from the product of particle pore volume, which is measured using nitrogen adsorption-desorption isotherms (77 K, Micromeritic Tristar 3000 analyzer) together with the density test.

2.6. Gas permeation test

The gas permeation testing rig is presented in Scheme 2. The gas permeation performance of the dense mixed matrix membranes was tested in a stainless steel flat sheet membrane permeation rig (effective area of 9.6 cm²). Prior to the test, the thickness of the membrane was measured using a micrometer. The membranes in this work had a

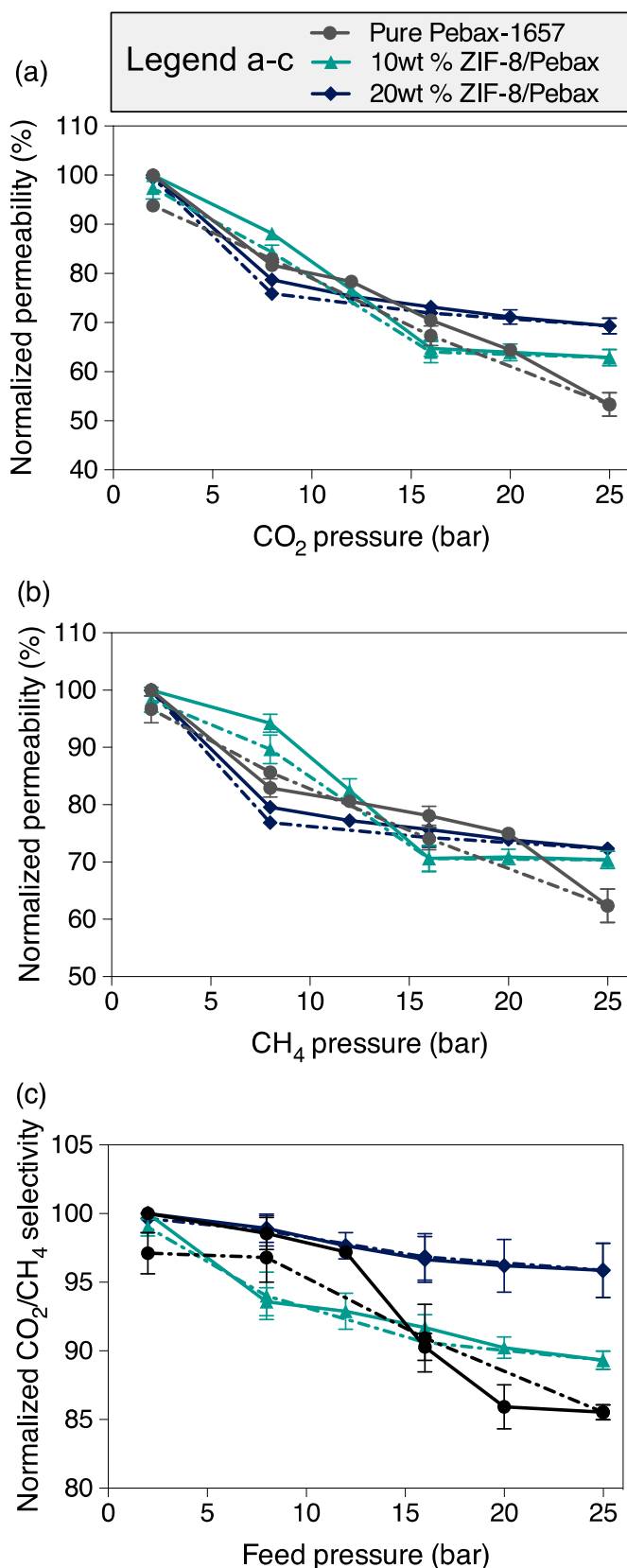


Fig. 5. Single gas permeation results of the ZIF-8/Pebax membrane at elevated pressure: (a) normalized CO₂ permeability, (b) normalized CH₄ permeability and (c) normalized selectivity of CO₂/CH₄. Solid line: pressurization; dash line: depressurization.

thickness of 50–60 μm . All gas permeation tests were carried out at room temperature (between 23 and 25 $^{\circ}\text{C}$), and the volumetric flow rate of gas in permeate was measured by a bubble flowmeter. For hollow fibre composite membranes, they were mounted in $\frac{1}{4}$ stainless steel membrane modules with an effective membrane area of 17 cm^2 . The pure gas permeability was calculated according to Eq. (4) below:

$$P = \frac{Q}{A \Delta p} \cdot x l \quad (4)$$

where P is the gas permeability, Q is the permeate volumetric flow rate (ml s^{-1}), Δp is pressure difference across the membrane (cmHg), A is membrane surface area (cm^2) and l is membrane thickness (cm).

The ideal selectivity of membrane for a given gas pair was determined from the ratio of the permeability of fast gas (A) to slow gas (B) based on Eq. (5):

$$\alpha = \frac{P_A}{P_B} \quad (5)$$

To investigate the influence of feed pressure on the membrane permeation performance, the experiments were conducted by monitoring the gas permeation under different feed pressure conditions. A complete test for each membrane contained a pressurization phase and a depressurization process phase. The tested pressured range was a 2–25 bar for flat sheet membranes and 2–15 bar for hollow fibre membranes. The feed gas pressure was increased and decreased stepwisely. Under each pressure condition, the membrane was exposed to feed gas for at least 1 h for sufficient equilibration and the permeability of CO₂ was firstly tested followed by CH₄ measurement under the same pressure condition, in order to understand the effect of the condensable gas on the permeation behaviour of the non-condensable gas.

In the mixed gas permeation test, CO₂/CH₄ (20/80, v/v) gas mixture was used as feed. The permeate composition was analysed with a Shimadzu gas chromatograph (Shimadzu GC-2014) equipped with a TCD detector and the mixed-gas permeability was calculated using Eq. (6):

$$\frac{P}{l} = \frac{Q Y_A}{a (p_x X_A - p_y Y_A)} \quad (6)$$

where p_x and p_y are the pressures of feed and permeate, a is the membrane area, and X and Y are the concentration in feed and permeate side. The selectivity of membrane for mixed-gas was calculated by following Eq. (7):

$$\alpha_{\frac{A}{B}} = \frac{Y_A/Y_B}{(p_x X_A - p_y Y_A)/(p_x X_B - p_y Y_B)} \quad (7)$$

In this work, the average of three gas permeation rate and selectivity results was reported.

3. Results and discussions

3.1. Characterization and performance of the mixed matrix membranes

3.1.1. Fabrication of ZIF-8 nanoparticles and mixed matrix membranes

In order to understand the mixed matrix membrane performance, two aspects need to be elucidated: dispersion of the particle fillers, and interfacial compatibility between polymer matrix and fillers [15]. Generally, nano-sized particles can be better dispersed within a polymer matrix, while the interfacial compatibility is determined by the surface functional groups. In this work, the ZIF-8 nanoparticles were in-house synthesized to mitigate the unwanted nanoparticle aggregation. The TEM images of the as-synthesized ZIF-8 particles are shown in Fig. 1a-b. They had rhombic dodecahedron morphology with a relatively minor agglomeration. Then the DLS particle sizer result indicates the average size was 72 nm with a polydispersity of

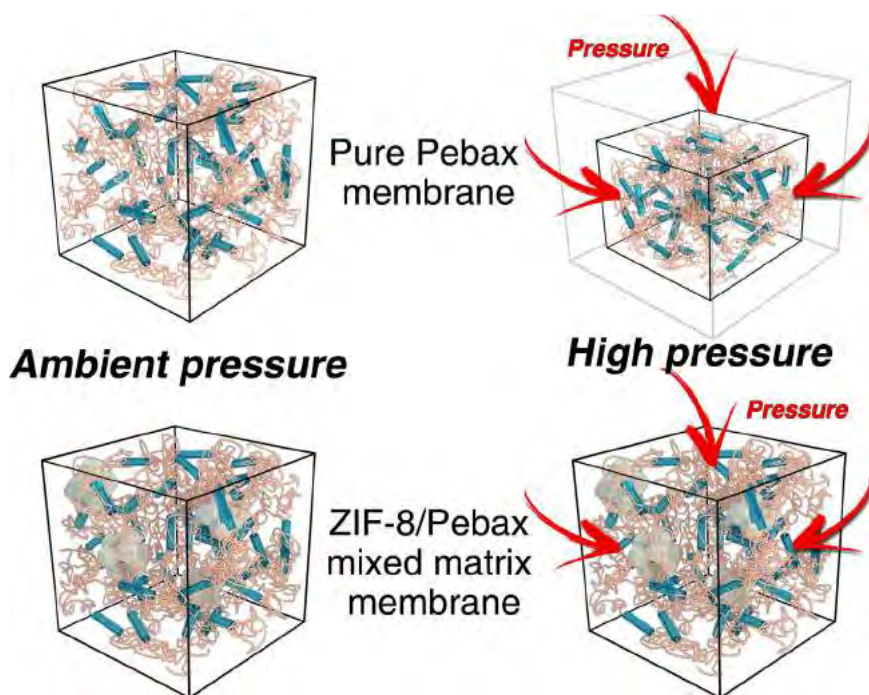


Fig. 6. Schematic representation of the polymeric structure of ZIF-8/Pebax mixed matrix membrane (plasticization is omitted for clarity).

0.17, which aligned the TEM images. Polydispersity is a dimensionless index to show the particle size dispersion. Normally a sample with polydispersity index lower than 0.05 can be regarded as highly monodispersed. This parameter is calculated by Cumulant method and given as $\frac{\Gamma_2}{\Gamma_1^2}$, where Γ_1 is related to gamma average of diffusion coefficient or the decay rate of the scattering light intensity and Γ_2 is the width of a probably distribution function of the diffusion coefficient [39]. The polydispersity value in this work is automatically calculated with the DLS software based on the obtained particle size distribution data. Furthermore, the nitrogen adsorption-desorption isothermal test shows the ZIF-8 nanoparticles had a BET surface area of $1,639 \text{ m}^2 \text{ g}^{-1}$ and a BJH pore volume of $0.8 \text{ cm}^3 \text{ g}^{-1}$, comparable to previous research results [34,40]. These findings confirm the porous framework structure of the prepared ZIF-8.

As shown in Fig. 1c-f, the surface and cross-section of pure Pebax membranes were smooth and continuous, and the ZIF-8 nanoparticles were well dispersed in the mixed matrix membrane without significant aggregation. However, the incorporation of 20 wt% ZIF-8 nanoparticles introduced some defects at the ZIF-8/Pebax interface region. We further conducted EDX tests on the membranes (Fig. S1). The clear Zn signal from the mixed matrix membrane confirmed the presence of ZIF-8 in the mixed matrix membrane, and the elemental mapping also suggested the even distribution of the ZIF-8 within the membrane.

3.1.2. Characterization of the mixed matrix membranes

To understand the performance of the mixed matrix membrane, comprehensive characterizations were carried out. Such information will also bridge the knowledge gap between dense flat sheet membranes and thin composite hollow fibre membranes. As discussed above, the performance of a mixed matrix membrane can be determined by the inherent properties of the organic matrix and the inorganic filler, as well as the interfacial interactions. The incorporation of ZIF-8 in the Pebax polymer can affect the polymer chain structure at the interfacial region [9]. We applied the DSC analysis to determine the glass transition (T_g) temperature of the membranes, which further reflected the degree of polymer chain flexibility [40,41]. For the pure Pebax copolymer, it should contain two distinct T_g for PEO (soft phase) and PA (hard phase) respectively. Based on our previous research, the

Pebax membrane fabricated with solvent evaporation technique had distinct microphase separation [7]. However, for the Pebax-1657 applied in this work only the T_g for PEO was detectable and the PA signal was too weak. As shown in Table 1, with the addition of ZIF-8, T_g of PEO was relatively unchanged. The presence of ZIF-8 could restrain the PEO chain movement at the interfacial region, but it may also create microvoids. These two effects result in the insignificant change in PEO chain flexibility after the incorporation of ZIF-8. The PEO T_g results here indicated a weak interaction between PEO section and ZIF-8 [42].

As presented in Table 2, the incorporation of ZIF-8 particles clearly reduced the membrane density and increased the fractional free volume (FFV). This can be partially attributed to the highly porous nature of the ZIF-8 nanoparticles. At the same time, it should be noted that the theoretical density calculated based on the pure material values was higher than the measured value: for example, the theoretical density of 20 wt% ZIF-8/Pebax was 1.09 g/cm^3 , compared to the 0.96 g/m^3 of measured value. This observation confirmed the incorporation of ZIF-8 created extra microvoids within the mixed matrix membrane, possibly due to the distortion of the original well-packed polymer chain structure [40].

In this work, BET analysis results showed very low surface areas of all membranes due to the dense-packed nature of the gas separation membranes. Still, the incorporation of ZIF-8 as porous filler increased the BET surface area of the membrane as shown in Table 2. However, considering the ultrahigh BET surface area of the pure ZIF-8, the incremental surface areas for the mixed matrix membranes were relatively minor, indicating most ZIF-8 were buried within the polymer matrix and barely accessible during the BET test.

The XRD patterns of the mixed matrix membrane can reflect the polymer and the nanofillers crystal structures. The narrow peak with high intensity represents the crystalline nature of the material, while the broad peak indicates the material is amorphous. As shown in Fig. 2a, the pure ZIF-8 had distinct peaks at 7.3° , 10.2° , 14.6° and 26.6° , which was in good agreement with the simulated and experimental XRD patterns of ZIF-8 [40,43]. Furthermore, the size of ZIF-8 can be calculated based on Scherrer Eq. (8)

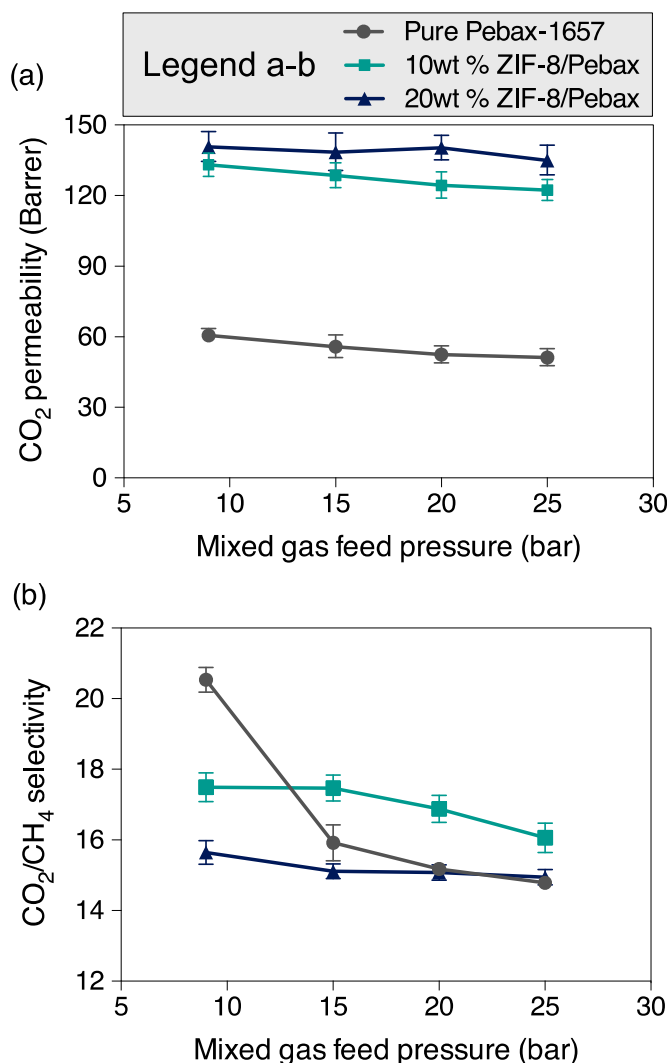


Fig. 7. (a) CO₂ permeability and (b) CO₂/CH₄ selectivity of Pebax-based membranes with mixed gas.

$$\tau = \frac{K\lambda}{\beta \cos\theta} \quad (8)$$

where τ is the mean size of the crystalline domains, K is the dimensionless shape factor, λ is the X-ray wavelength, β is the line broadening at half the maximum intensity, and θ is the Bragg angle. The calculated ZIF-8 had an average crystalline domain size of ~80 nm, which was in good agreement with previous DLS results.

The XRD patterns of the pure Pebax containing both rubbery PEO and glassy PA phases (Fig. 2a) illustrated the distinct peak at 24.1° (crystalline PA phases) and the broader peak ranging from 17.5° to 22.5° (amorphous phase or soft phase) [44]. For the mixed matrix membranes (Fig. 2b), the ZIF-8 pattern was relatively unchanged, indicating that the crystalline structure was preserved. On the other hand, with the increase of ZIF-8 loading the crystalline, PA peak became more obvious accompanied with the loss of amorphous peaks (PEO section). In addition, the XRD pattern also suggested the ZIF-8 within Pebax polymers had no preferred orientation.

We further calculated the membrane crystallinity from both DSC and XRD results. From the DSC results, the crystallinity (X_c) in both soft and hard phase was estimated using the Eq. (8):

$$X_c = \frac{\Delta H_m}{\Delta H_m^0} \quad (8)$$

where the melting enthalpy (ΔH_m) was estimated from the area of the

melting peak in the DSC curves, and the melting enthalpy of the pure crystalline phase (ΔH_m^0) of PEO was 166.4 J/g and PA was 230 J/g, which was adapted from literature [45,46]. The membrane crystallinity from XRD analysis was calculated by taking the ratio of the area of the crystalline region and the total area of crystalline and amorphous region on the XRD patterns.

From Table 1, the degree of crystallinities derived from DSC and XRD analysis were comparable. The degree of crystallinity of pure Pebax membrane was around 16–17%. After the incorporation of the ZIF-8 particle, the crystallinity of both PEO and PA phases increased simultaneously.

The addition of ZIF-8 disrupted the original interchain hydrogen bonds with the polymer matrix. At the same time, it led to the formation of new secondary chemical bonding at the interfacial region [47]. Based on our previous research, the fabricated Pebax-1657 flat sheet membrane contained distinct hard and soft domains due to the microphase separation: the hard domains had a rod-like shape with a length of ~100 nm, interspaced with flexible amorphous soft phase (Fig. 3a) [7]. Considering their comparable dimensions, the hard domain (PA section) could have intimate contact with the added ZIF-8 in this work (80 nm in diameter), which further facilitated the formation of extra hydrogen bonds between aldehyde groups (PA) and methyl groups (ZIF-8), methyl protons of 2-methylimidazole and amide carbon, as well as between the N-H groups (PA) and N atoms on imidazole rings (ZIF-8) [48,49]. The rigid PA and ZIF-8, together with the extra hydrogen bonds, could stabilize the composite polymer/ZIF-8 structure. However, this would also reduce the original packing density of the amorphous PEO section, leading to a weaker internal interaction within the PEO chains and increased free volume within the mixed matrix membranes (Fig. 3b-c).

FT-IR analysis was conducted to further investigate the formation of hydrogen bonds between ZIF-8 particles and Pebax polymer chains. The spectra are presented in Fig. 3d-f. For the pure Pebax membrane, the distinct peak at around 1094 cm⁻¹ is attributed to the stretching vibration of C-O-C group within the PEO segment. The polyamide block in Pebax-1657 shows relatively sharp peaks at around 3297, 1636 and 1730 cm⁻¹. These three peaks are attributed to the -N-H-, H-N-C=O and O-C=O groups in the hard polyamide segment [50,51]. The incorporation of ZIF-8 particles into polymer matrix leads to the shift in peak wavenumber for -N-H-, H-N-C=O and O-C=O groups (Fig. 3e-f). The peak shifts for the functional groups in hard segment of Pebax confirm the formation of hydrogen bonds between ZIF-8 and polyamide segment, and similar phenomenon has been observed for Pebax and UiO₆₆-NH₂ mixed matrix membranes [50]. In comparison, the PEO peak is relatively unchanged for the mixed matrix membranes, indicating the relatively weak interactions between ZIF-8 and PEO sections. Such an observation aligns the previous DSC results.

3.1.3. Gas separation performance of ZIF-8/Pebax mixed matrix membrane

Gas permeability of the mixed matrix membranes was significantly higher than the pure Pebax benchmark, but it was accompanied with the slight loss of selectivity (Fig. 4, Table 3 and Fig. S2). Specifically, for the pure Pebax benchmark the CO₂ permeability was much higher than the other tested gases, which could be attributed to the rubbery PEO block in Pebax having a strong affinity to the polar gas (CO₂) over the non-polar gases (N₂, O₂ and CH₄) [52]. After the incorporation of ZIF-8, its selective adsorption of CO₂ onto the organic ligands improved the dissolution of CO₂ in the mixed matrix membranes (Fig. S3) [40]. On the other hand, as discussed previously, the presence of ZIF-8 created extra micro-voids at the interface, and it has been reported that the flexible structure of ZIF-8 could form non-selective flow channels for CO₂ and N₂ [40,53]. These contradicting effects led to the higher permeability and lower selectivity for the mixed matrix membranes. As presented above, the mixed matrix membranes had significantly higher FFV compared with the pure Pebax benchmark (Table 2).

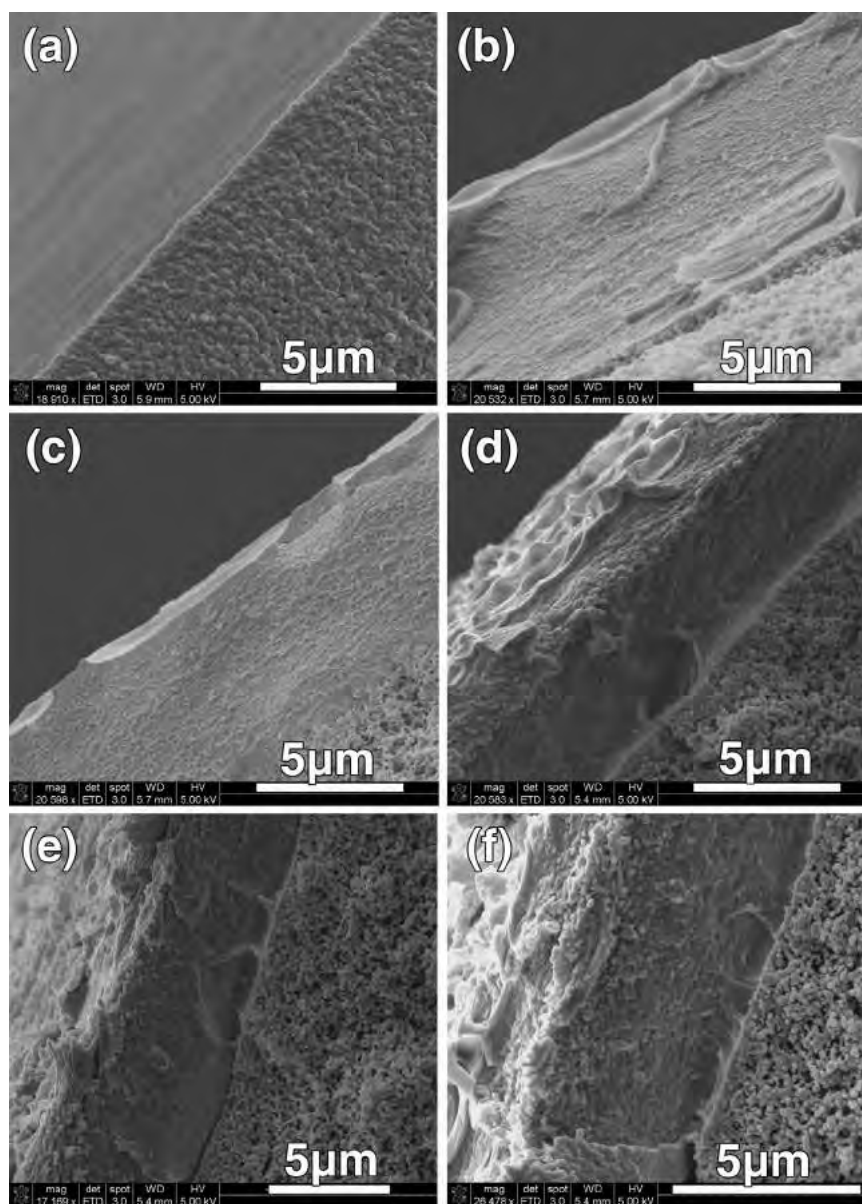


Fig. 8. Cross-sectional SEM images of (a) pristine PVDF, (b) PTMSP coated membrane, composite membranes with (c) pure Pebax, (d) 10 wt% ZIF-8/Pebax selective layer, (e) 20 wt% ZIF-8/Pebax selective layer, and (f) 30 wt% ZIF-8/Pebax selective layer.

However, their selectivity loss was relatively minor (~15%). The derivation between permeability and the free volume suggests the interaction between polar gas and PEO groups still dominated the gas transport through the mixed matrix membranes.

3.2. High-pressure performance of the ZIF-8/Pebax mixed matrix membrane

3.2.1. High-pressure pure gas test

Polymeric membrane plasticization is a challenging issue for the glassy polymer materials. However, the performance of Pebax-based membranes under an elevated pressure have not been fully elucidated [54]. In this work, we exposed the Pebax-based membranes to a complete pressurization-depressurization cycle (up to 25 bar) to investigate the effect of high-pressure feed on the membrane performance. In addition, we also investigated the CH₄ permeation rate upon the completion of CO₂ permeation under each pressure condition.

As shown in Fig. 5a, the CO₂ gas permeation results suggested a different behaviour of the phase separated copolymer membranes

compared with the glassy polymer membranes [41,55,56]. Within the tested pressure range, the CO₂ permeability decreased with higher CO₂ feed pressure for both pure Pebax and ZIF-8/Pebax mixed matrix membranes. The most significant decrease was observed with the pure Pebax membrane, and the addition of ZIF-8 reduced the loss of CO₂ permeability under high feed pressure. As the transport of gas through the Pebax membrane occurred mainly through the soft phase segments [7,52], the effect of pressure on the gas permeability can be rationalized by the competing effects of hydrostatic pressure and plasticization: although more CO₂ was absorbed with higher feed pressure, the membrane free volume was also reduced due to the compaction effect [7,52]. In addition, the Pebax-based flat sheet membranes in this work did not show significant plasticization under up to 25 bar of CO₂ and further depressurization process fully resumed the CO₂ permeability for all tested membranes, indicating the reversible compaction behaviour of the membranes.

Polymer chain compaction under high pressure also influenced the permeability of CH₄. As presented in Fig. 5b, the increased feed pressure led to a lower CH₄ permeability. In terms of the ideal CO₂/

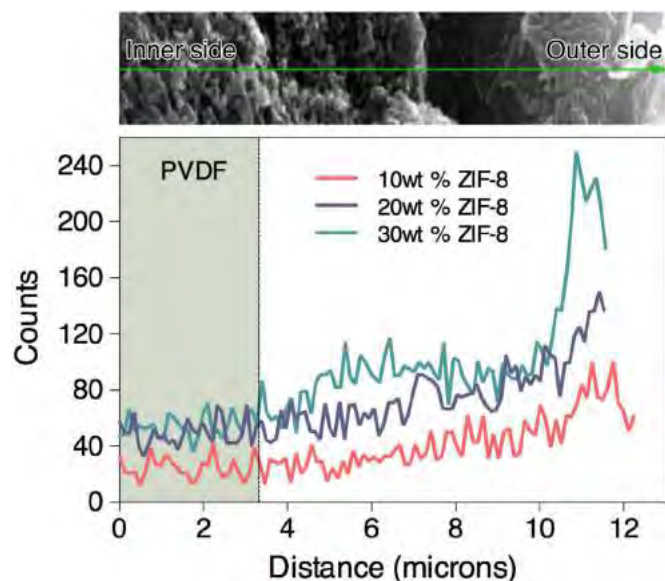


Fig. 9. EDX line scan of Zn element along the cross-sectional direction of ZIF-8/Pebax-1657 composite membranes.

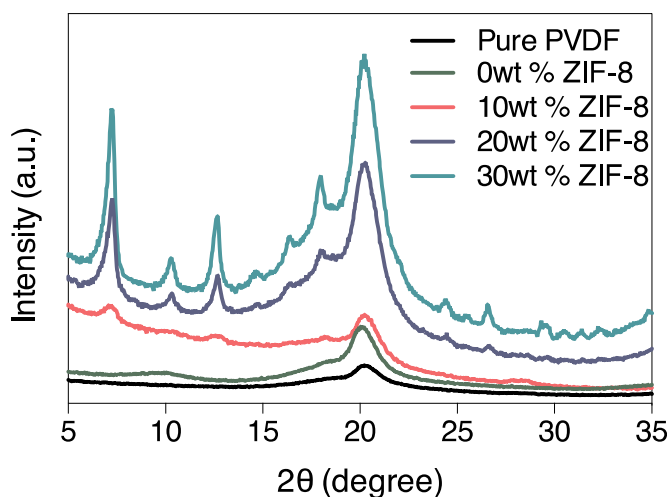


Fig. 10. XRD spectra of Pure PVDF and composite membranes with various ZIF-8 loadings.

CH₄ selectivity, the selectivity for pure Pebax reduced to 85% of its original level at 25 bar while for the mixed matrix membranes the selectivity was relatively stable (Fig. 5c), and the selectivity can be fully recovered at the end of the depressurization phase. A schematic model representing the effect of compaction on polymer structure is shown in Fig. 6. As a block copolymer, Pebax is built from soft PEO and hard PA phases. Based on the XRD results (Fig. 2), the formation of hydrogen bonds between PA and ZIF-8 rigidified the glassy PA section. Together with its good mechanical properties, the incorporation of ZIF-8 improved the polymer structural stability especially under high pressure.

3.2.2. High-pressure mixed gas test

The membrane permeation behaviour with the mixed gas can be different from the pure gas due to the competitive sorption and the concentration polarization [10,57,58]. In this work, the high-pressure permeation tests with mixed gas (20/80, CO₂/CH₄) were conducted to simulate the industrial natural gas sweetening process, and up to 25 bar of feed pressure was applied. The membranes were exposed to the mixed gas for 1 h at each pressure prior to the permeation data collection.

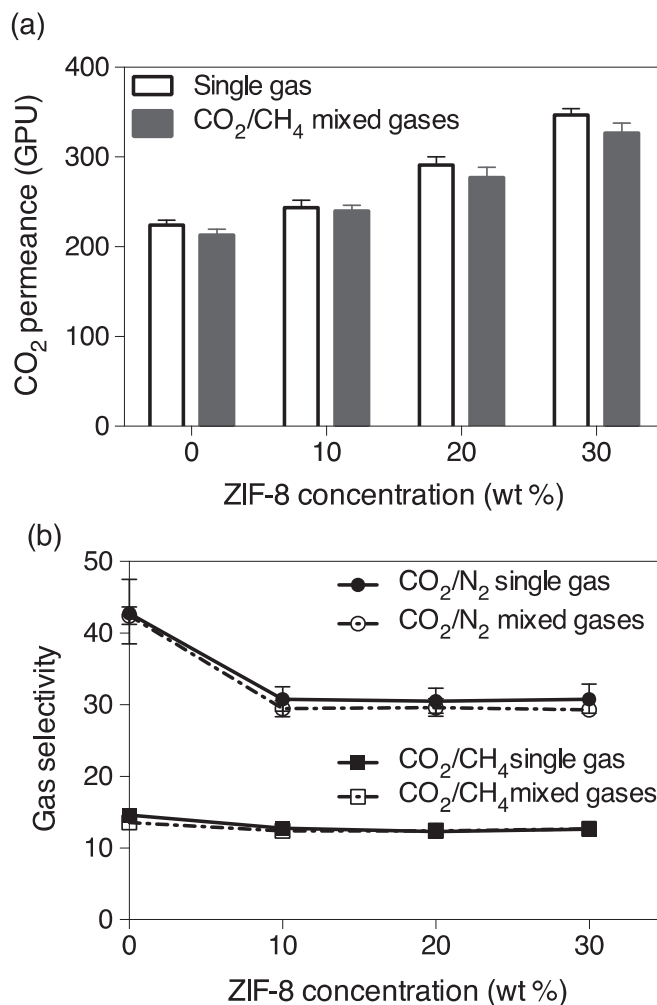


Fig. 11. CO₂ gas permeance and gas selectivity of ZIF-8/Pebax-1657 based hollow fibre composite membranes (pure gas selectivity is represented by solid line and mixed gases selectivity is represented by dash line).

The membrane performance with mixed gas is presented in Fig. 7. The CO₂ permeability for all tested membranes were slightly lower compared with the pure gas results (Fig. 7a). Similarly, with the increase of feed pressure, reduced permeability was observed due to the competitive sorption and the polymer chain compaction [59]. No significant plasticization of the Pebax-based membranes was observed within the tested pressure range.

In terms of the selectivity (Fig. 7b), with the increase of feed pressure, a significant reduction of CO₂/CH₄ selectivity was observed with the pure Pebax membrane. In comparison, the selectivity for the mixed matrix membranes was relatively unchanged. This observation aligned previous pure gas results, and the more stable selectivity for the mixed matrix membranes could be attributed to higher diffusion rate of CO₂ over CH₄ within the ZIF-8 structure, the CO₂ adsorption near the pore aperture of ZIF-8 hindered the CH₄ diffusion through the crystal, as well as more rigid polymer chains as presented above [40,41].

3.3. ZIF-8/Pebax hollow fibre composite membranes

The mixed matrix membranes that combine metal organic framework and polymer matrix showed a good potential of efficient gas separation under elevated pressure. For industrial application, a composite hollow fibre membrane with a thin selective layer is preferable due to their higher practical permeation rate and easier scale-up. However, the behaviour of the thin composite layer under high pressure feed gas condition has not been fully understood. In this

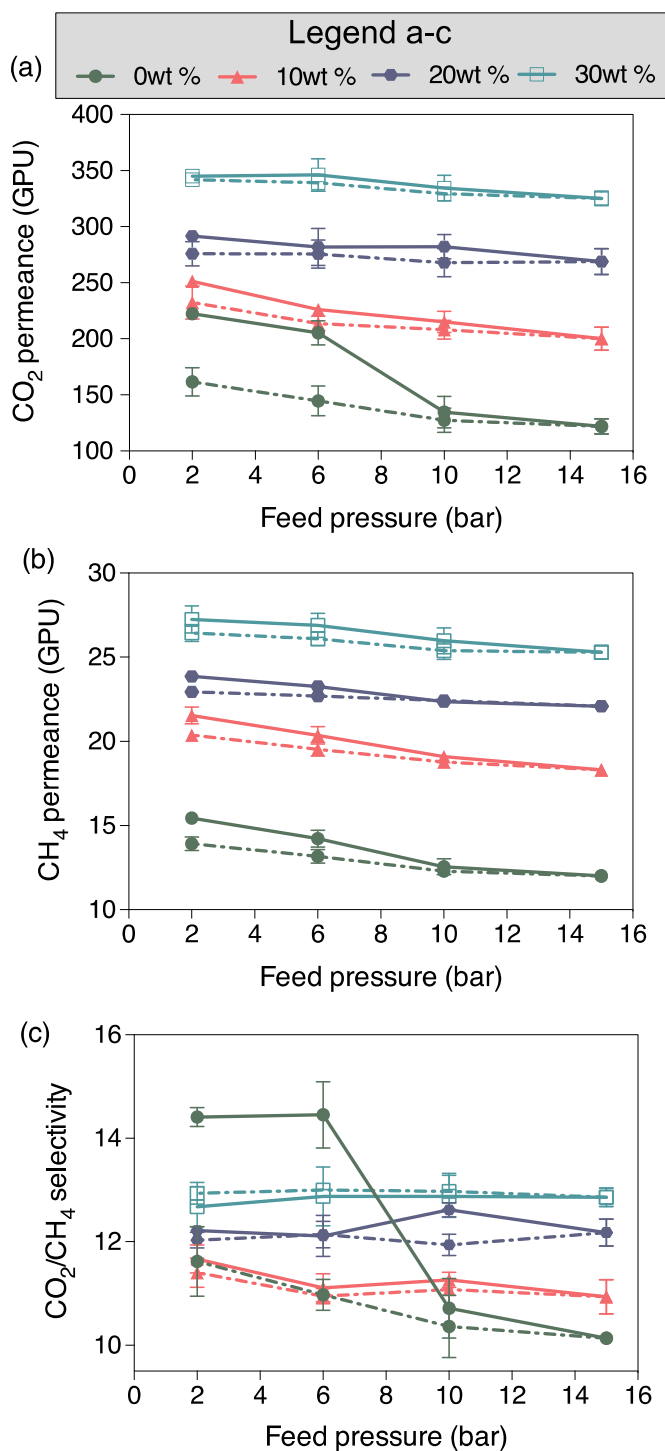


Fig. 12. High-pressure gas permeation results of ZIF-8/Pebax-1657 hollow fibre composite membranes: (a) CO₂ permeance, (b) CH₄ permeance and (c) CO₂/CH₄ gas ideal selectivity. Solid line: pressurization; dash line: depressurization.

work, we pre-coated the PVDF membrane with a gutter layer of highly permeable polymer. This smooth gutter layer can prevent the intrusion of Pebax into supportive membrane pores, ensuring a thin and continuous selective layer [4]. Both PDMS and PTMSP gutter layers were compared (Table S1), and PTMSP clearly had higher permeance and selectivity. As a result, except where otherwise noted, composite membranes with PTMSP gutter were used for the subsequent tests.

3.3.1. Morphology of composite membrane

As shown in Fig. 8, the PTMSP gutter layer thickness was around

7 μm. Subsequently, the deposition of Pebax selective and protective layer increased the whole coating layer thickness by ~1.5 μm. However, it is difficult to precisely determine the Pebax layer thickness due to the lack of a distinct interface between PTMSP and Pebax layers. This suggested that during the Pebax dip-coating process, the PTMSP gutter layer was partially re-dissolved by solvent, which led to stronger adhesion between the Pebax and the PTMSP layers, and was beneficial for the composite membrane stability. This observation was in agreement with other researches on composite membranes [4,25].

The membrane surface roughness increased with higher ZIF-8 loading in the thin Pebax layer, indicating the formation of particle aggregation (Fig. 8d-f). The coating layer thickness was relatively unchanged for Pebax with different ZIF-8 loadings. Further EDX line scan graph shows the Zn distribution from inner to outer side of the membrane (Fig. 9), and the distribution profiles aligned the SEM images that the selective layer was around 1.5 μm in thickness.

3.3.2. Crystallinity and thermal properties of composite membranes

The XRD spectra of the as-synthesized ZIF-8 particle, pure PVDF porous support and nanocomposite membrane with various ZIF-8 particles loadings are presented in Fig. 10. The XRD pattern of PVDF support shows an obvious peak at $2\theta=21^\circ$, indicating that the PVDF substrate was in its semi-crystalline phase [60]. In terms of the composite membrane with pure Pebax, the signature peak at 10° can be assigned to the glassy PTMSP gutter layer [31]. However, the peak of glassy PA in Pebax was not detectable, possibly due to the Pebax coating amount was relatively small. In terms of the composite membranes containing ZIF-8, the original crystallinity of ZIF-8 was well preserved, and peak intensity increased with higher ZIF-8 loading.

We further conducted the DSC analysis to investigate the effect of ZIF-8 on the thermal properties of the composite membranes. However, the DSC patterns of the composite membrane were relatively unchanged compared with the pure PVDF benchmark (Fig. S4), indicating the characterization technique was not sensitive enough to detect the thermal properties of the thin coating layer.

3.3.3. Gas separation performance of ZIF-8/Pebax hollow fibre composite membrane

Gas separation tests of the ZIF-8/Pebax-based composite membrane was carried out with both pure gas and mixed gas at room temperature with 2 bar feed pressure. Based on the flat sheet membrane results, the incorporation of ZIF-8 nanoparticles significantly improved the gas permeability while only led to a marginal loss of the selectivity (Section 3.1.3). Similar gas separation results were also observed with the composite membranes as shown in Fig. 11, and permeation flow rates for the composite membrane were significantly higher than the thick flat sheet membranes (Fig. S2). As discussed above, the incorporation of ZIF-8 increased the FFV for the dense membranes (Table 2), and a strong interaction was observed between ZIF-8 and glassy PA section (XRD results in Fig. 2). Both aspects could lead to the formation of defects within the thin composite selective layer. However, based on the gas permeation results, the microvoids at the ZIF-8/Pebax interfacial region were still relatively minor and non-continuous, even with the highest ZIF-8 loading in this work (30 wt%). This observation was especially preferable for the scale-up of the composite hollow fibre membrane, due to the ease of minimizing defects. In addition, the composite membranes had comparable performance with both pure and mixed feed gas: the adsorption of polar gas (CO₂) onto ZIF-8 prevented the permeation of CH₄ and N₂, which was beneficial to the membrane selectivity [40]. This observation suggested the good potential of the composite membrane for practical application. In addition, we also fabricated the composite membrane with PDMS gutter, but their permeance and selectivity were both lower compared with PTMSP counterparts, indicating the poor compatibility between Pebax and PDMS gutter layer (Table S2).

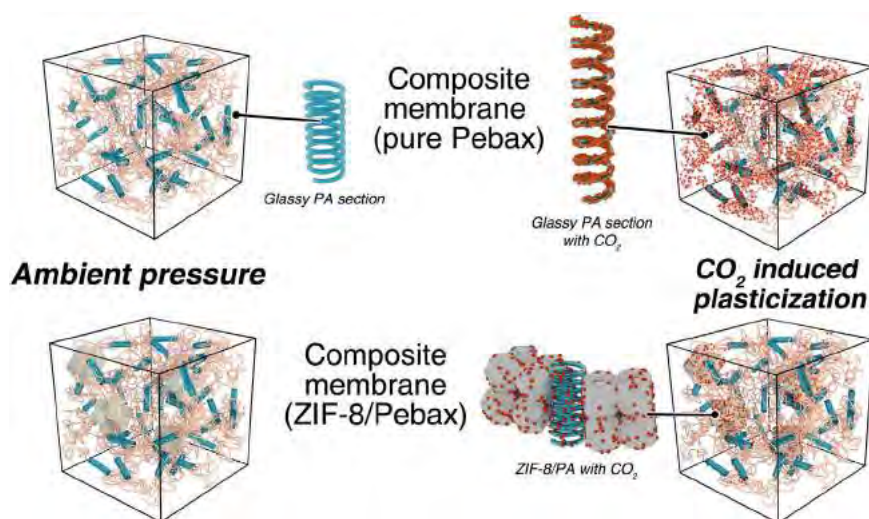


Fig. 13. Schematic representation of the plasticization of the composite membrane selective layer (compaction is omitted for clarity).

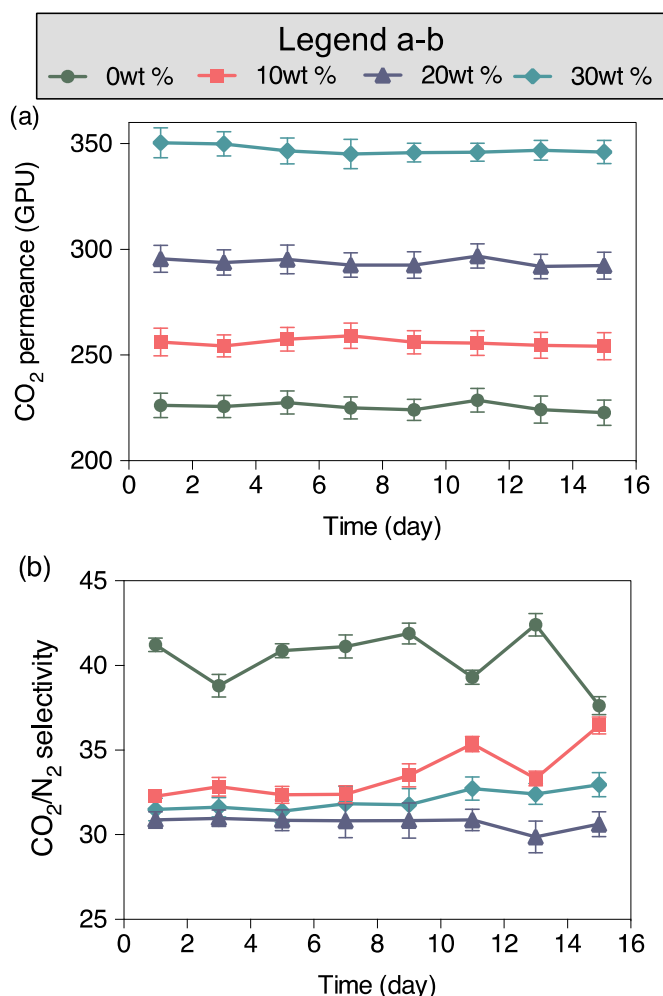


Fig. 14. Operational stability of ZIF-8/Pebax hollow fibre composite membrane: (a) CO₂ gas permeance and (b) CO₂/N₂ gas selectivity.

3.3.4. Gas separation performance with pressurization-depressurization steps

A highly efficient membrane with good plasticization/compaction resistance can be a promising candidate for high-pressure natural gas sweetening and hydrogen purification, as CO₂ can be directly removed from the high-pressure feed, which does not require the re-pressuriza-

tion of the purified CH₄ or H₂ [61–63]. However, most thin composite membranes have only been investigated under relatively low pressure [22,27,64,65]. Compared with the dense flat sheet membrane, the thin composite membrane could be more susceptible to the pressure-induced plasticization/compaction effect due to their relatively inferior mechanical properties. In this work, we investigated the performance of composite hollow fibre membrane under elevated pressure conditions (equilibrium time of 1 h under each pressure condition). It should be noted that the highest pressure tested was 15 bar, as further increase the feed pressure led to the collapse of the supporting PVDF membrane. In terms of the pure Pebax-coated membrane (Fig. 12a), a pressure-induced compaction effect was observed: high feed pressure led to the loss of CO₂ permeation rate, and after the depressurization cycle only partial of the original CO₂ permeation rate was recovered. Together with the loss of CO₂/CH₄ selectivity at the end of the test (Fig. 12b-c), these results indicated the pressurization-depressurization cycle led to plasticization and irreversible compaction. As demonstrated in the Section 3.1.3, the gas permeation through Pebax was dominated by the rubbery PEO section. However, the condensation of CO₂ on the glassy PA section increased the glassy chain mobility and led to lower selectivity for the thin Pebax layer [7].

On the other hand, the incorporation of ZIF-8 nanoparticles helped to reduce the plasticization/compaction effect. The permeation rate and selectivity were more stable within the whole tested pressure range (Fig. 12). Based on our previous discussion (Section 3.1.2), the strong interaction between ZIF-8 and glassy PA section improved the structural stability of the Pebax layer, leading to improved compaction resistance. At the same time, the hydrogen bonds between ZIF-8 and PA occupied the CO₂ adsorptive sites on the PA chains (polar functional groups like C=O and C-N-C), and the hydrogen bond provided extra support which improved the swelling resistance of the PA chains. In addition, the ZIF-8 framework structure also provided high CO₂ absorptive capacity. All these factors suppressed the CO₂-induced plasticization for the PA chains (Fig. 13).

3.3.5. Long-term stability of ZIF-8/Pebax based composite hollow fibre membrane

Lastly, we investigated the stability of the composite membrane. PTMSP was used as a gutter layer for the composite membrane, and one major concern is its aging. The gradual relaxation of the non-equilibrium porous glassy polymer chains can lead to a significant loss of the permeance. For example, 80% of the CO₂ permeance can be lost for a thin PTMSP coating layer within 14 days [4]. Furthermore, it has been demonstrated that the PTMSP aging can be progressively accelerated with the decrease of its thickness [66]. In this work, the

composite membrane performance was relatively stable for 15 days (Fig. 14), indicating the PTMSP aging was negligible. In comparison, the membrane with bare PTMSP gutter layer experienced over 22% loss of CO₂ permeance within the same time (results not shown). As shown in Fig. 8, the Pebax coating layer was partially permeated into the PTMSP gutter layer, indicating their polymer chains could be intertwined, which stabilized the non-equilibrium PTMSP structure. This could provide a facile approach to mitigate the aging of the highly porous glassy polymers and facilitate the large-scale membrane fabrication. The detailed PTMSP anti-aging mechanism within the composite membrane is beyond the scope of the current work and will be investigated in our subsequent studies.

4. Conclusions

In this work, ZIF-8/Pebax-1657 based dense flat sheet mixed matrix membranes and hollow fibre composite membranes were fabricated and examined. The addition of ZIF-8 into the Pebax matrix improved the gas permeance for all membranes, accompanied with only slightly loss of gas selectivity. The flat sheet membrane characterization results indicated the formation of hydrogen bonds between 2-methylimidazole and PA section, which improved the rigidity of the whole ZIF-8/Pebax structure. As a result, the improved compaction/plasticization resistance was observed with both flat sheet and hollow membranes based on the complete pressurization-depressurization test. In addition, the long-term operational performance of the composite membrane suggested the ZIF-8/Pebax coating layer could stabilize the highly porous glassy PTMSP gutter layer structure. This work bridged the knowledge gap between flat sheet membrane characterization results and hollow fibre composite membrane performance, and the ZIF-8/Pebax based hollow fibre composite membrane could be a potential candidate for industrial application due to its good operational stability. But this is subject to further investigation of the membrane performance under harsh industrial gas separation conditions (such as the presence of SO_x, NO_x, and water vapour).

Acknowledgements

This work was supported by UNSW Goldstar Award and Scientific and Industry Endowment Fund in Australia (SIEF Grant ID RP02-035) (CO2MOF). Putu Doddy Sutrisna would also like to acknowledge Australia Awards for the scholarship provided.

Appendix A. Supplementary material

Supplementary data associated with this article can be found in the online version at doi:10.1016/j.memsci.2016.11.048.

References

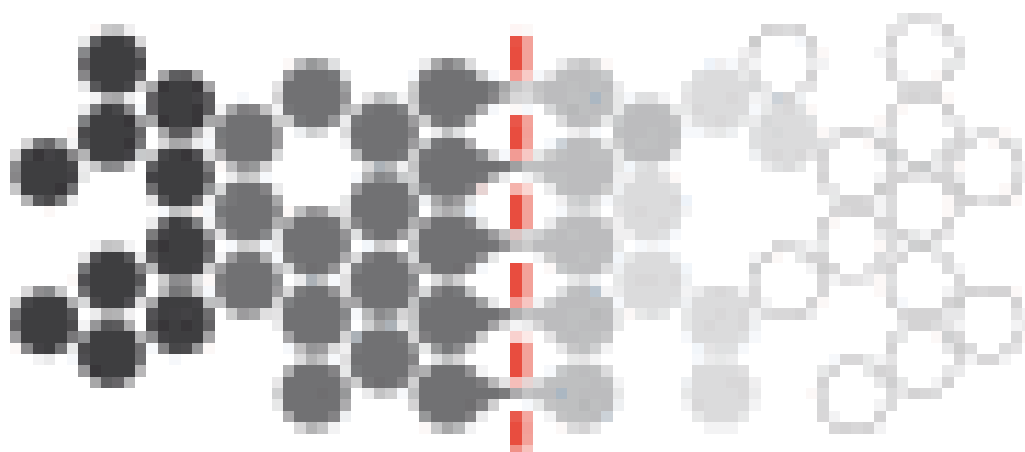
- [1] S. Zhao, P.H.M. Feron, L. Deng, E. Favre, E. Chabanon, S. Yan, J. Hou, V. Chen, H. Qi, Status and progress of membrane contactors in post-combustion carbon capture: a state-of-the-art review of new developments, *J. Membr. Sci.* 511 (2016) 180–206.
- [2] Y. Zhang, R. Wang, Gas–liquid membrane contactors for acid gas removal: recent advances and future challenges, *Curr. Opin. Chem. Eng.* 2 (2013) 255–262.
- [3] J. Hou, G. Dong, B. Xiao, C. Malassigne, V. Chen, Preparation of titania based biocatalytic nanoparticles and membranes for CO₂ conversion, *J. Mater. Chem. A* 3 (2015) 3332–3342.
- [4] H.Z. Chen, Z. Thong, P. Li, T.-S. Chung, High performance composite hollow fiber membranes for CO₂/H₂ and CO₂/N₂ separation, *Int. J. Hydrog. Energy* 39 (2014) 5043–5053.
- [5] J. Hou, P.D. Sutrisna, Y. Zhang, V. Chen, Formation of ultrathin, continuous metal–organic framework membranes on flexible polymer substrates, *Angew. Chem. Int. Ed.* 55 (2016) 3947–3951.
- [6] A.J. Brown, N.A. Brunelli, K. Eum, F. Rashidi, J.R. Johnson, W.J. Koros, C.W. Jones, S. Nair, Interfacial microfluidic processing of metal-organic framework hollow fiber membranes, *Science* 345 (2014) 72–75.
- [7] Y. Wang, H. Li, G. Dong, C. Scholes, V. Chen, Effect of fabrication and operation conditions on CO₂ separation performance of PEO–PA block copolymer membranes, *Ind. Eng. Chem. Res.* 54 (2015) 7273–7283.
- [8] G. Dong, Y. Zhang, J. Hou, J. Shen, V. Chen, Graphene oxide nanosheets based novel facilitated transport membranes for efficient CO₂ capture, *Ind. Eng. Chem. Res.* 55 (2016) 5403–5414.
- [9] G. Dong, H. Li, V. Chen, Challenges and opportunities for mixed-matrix membranes for gas separation, *J. Mater. Chem. A* 1 (2013) 4610–4630.
- [10] G. Dong, H. Li, V. Chen, Plasticization mechanisms and effects of thermal annealing of Matrimid hollow fiber membranes for CO₂ removal, *J. Membr. Sci.* 369 (2011) 206–220.
- [11] S. Kim, Y.M. Lee, Rigid and microporous polymers for gas separation membranes, *Prog. Polym. Sci.* 43 (2015) 1–32.
- [12] L.M. Robeson, Correlation of separation factor versus permeability for polymeric membranes, *J. Membr. Sci.* 62 (1991) 165–185.
- [13] L.M. Robeson, Q. Liu, B.D. Freeman, D.R. Paul, Comparison of transport properties of rubbery and glassy polymers and the relevance to the upper bound relationship, *J. Membr. Sci.* 476 (2015) 421–431.
- [14] L.M. Robeson, The upper bound revisited, *J. Membr. Sci.* 320 (2008) 390–400.
- [15] H.-C. Yang, J. Hou, V. Chen, Z.-K. Xu, Surface and interface engineering for organic-inorganic composite membranes, *J. Mater. Chem. A* 4 (2016) 9716–9729.
- [16] S. Shahid, K. Nijmeijer, Performance and plasticization behavior of polymer–MOF membranes for gas separation at elevated pressures, *J. Membr. Sci.* 470 (2014) 166–177.
- [17] J.A. Thompson, J.T. Vaughn, N.A. Brunelli, W.J. Koros, C.W. Jones, S. Nair, Mixed-linker zeolitic imidazolate framework mixed-matrix membranes for aggressive CO₂ separation from natural gas, *Microporous Mesoporous Mater.* 192 (2014) 43–51.
- [18] S.R. Venna, M. Lartey, T. Li, A. Spore, S. Kumar, H.B. Nulwala, D.R. Luebke, N.L. Rosi, E. Albenze, Fabrication of MMMs with improved gas separation properties using externally-functionalized MOF particles, *J. Mater. Chem. A* 3 (2015) 5014–5022.
- [19] Z. Wang, D. Wang, S. Zhang, L. Hu, J. Jin, Interfacial design of mixed matrix membranes for improved gas separation performance, *Adv. Mater.* 28 (2016) 3399–3405.
- [20] S. Shahid, K. Nijmeijer, High pressure gas separation performance of mixed-matrix polymer membranes containing mesoporous Fe(BTC), *J. Membr. Sci.* 459 (2014) 33–44.
- [21] M. Rezakazemi, A. Ebadi Amooghin, M.M. Montazer-Rahmati, A.F. Ismail, T. Matsuura, State-of-the-art membrane based CO₂ separation using mixed matrix membranes (MMMs): an overview on current status and future directions, *Prog. Polym. Sci.* 39 (2014) 817–861.
- [22] A. Jomekian, R.M. Behbahani, T. Mohammadi, A. Kargari, CO₂/CH₄ separation by high performance co-casted ZIF-8/Pebax 1657/PES mixed matrix membrane, *J. Nat. Gas Sci. Eng.* 31 (2016) 562–574.
- [23] H.-C. Yang, J. Hou, V. Chen, Z.-K. Xu, Janus membranes: exploring duality for advanced separation, *Angew. Chem. Int. Ed.* 55 (2016) 13398–13407.
- [24] Q. Fu, J. Kim, P.A. Gurr, J.M.P. Scofield, S.E. Kentish, G.G. Qiao, A novel cross-linked nano-coating for carbon dioxide capture, *Energy Environ. Sci.* 9 (2016) 434–440.
- [25] Q. Fu, E.H.H. Wong, J. Kim, J.M.P. Scofield, P.A. Gurr, S.E. Kentish, G.G. Qiao, The effect of soft nanoparticles morphologies on thin film composite membrane performance, *J. Mater. Chem. A* 2 (2014) 17751–17756.
- [26] A. Halim, Q. Fu, Q. Yong, P.A. Gurr, S.E. Kentish, G.G. Qiao, Soft polymeric nanoparticle additives for next generation gas separation membranes, *J. Mater. Chem. A* 2 (2014) 4999–5009.
- [27] J. Kim, Q. Fu, K. Xie, J.M.P. Scofield, S.E. Kentish, G.G. Qiao, CO₂ separation using surface-functionalized SiO₂ nanoparticles incorporated ultra-thin film composite mixed matrix membranes for post-combustion carbon capture, *J. Membr. Sci.* 515 (2016) 54–62.
- [28] J. Kim, Q. Fu, J.M.P. Scofield, S.E. Kentish, G.G. Qiao, Ultra-thin film composite mixed matrix membranes incorporating iron(III)-dopamine nanoparticles for CO₂ separation, *Nanoscale* 8 (2016) 8312–8323.
- [29] P. Li, Z. Wang, W. Li, Y. Liu, J. Wang, S. Wang, High-performance multilayer composite membranes with mussel-inspired polydopamine as a versatile molecular bridge for CO₂ separation, *ACS Appl. Mater. Interfaces* 7 (2015) 15481–15493.
- [30] C.H. Lau, P.T. Nguyen, M.R. Hill, A.W. Thornton, K. Konstas, C.M. Doherty, R.J. Mulder, L. Bourgeois, A.C.Y. Liu, D.J. Sprouster, J.P. Sullivan, T.J. Bastow, A.J. Hill, D.L. Gin, R.D. Noble, Ending aging in super glassy polymer membranes, *Angew. Chem. Int. Ed.* 53 (2014) 5322–5326.
- [31] A. Fernández-Barquín, C. Casado-Coterillo, M. Palomino, S. Valencia, A. Irbabien, LTA/Poly(1-trimethylsilyl-1-propyne) mixed-matrix membranes for high-temperature CO₂/N₂ separation, *Chem. Eng. Technol.* 38 (2015) 658–666.
- [32] M. Kitchin, J. Teo, K. Konstas, C.H. Lau, C.J. Sumbly, A.W. Thornton, C.J. Doonan, M.R. Hill, AIMS: a new strategy to control physical aging and gas transport in mixed-matrix membranes, *J. Mater. Chem. A* 3 (2015) 15241–15247.
- [33] N.R. Horn, D.R. Paul, Carbon dioxide plasticization and conditioning effects in thick vs. thin glassy polymer films, *Polymer* 52 (2011) 1619–1627.
- [34] J. Cravillon, S. Münzer, S.-J. Lohmeier, A. Feldhoff, K. Huber, M. Wiebecke, Rapid room-temperature synthesis and characterization of nanocrystals of a prototypical zeolitic imidazolate framework, *Chem. Mater.* 21 (2009) 1410–1412.
- [35] B.D. Freeman, I. Pinnau, Polymeric materials for gas separations, in: B.D. Freeman, I. Pinnau (Eds.), *Polymer Membranes for Gas and Vapor Separation: Chemistry and Material Science*, American Chemical Society, Washington, DC, 1999, pp. 1–27.
- [36] R.W. Baker, *Membrane Technology and Applications*, second edition, John Wiley & Sons Ltd, West Sussex, England, 2004.
- [37] A. Bondi, *Physical Properties of Molecular Crystals, Liquids, and Glasses*, John

- Wiley & Sons, New York, 1968.
- [38] S. Kanehashi, G.Q. Chen, C.A. Scholes, B. Ozcelik, C. Hua, L. Ciddor, P.D. Southon, D.M. D'Alessandro, S.E. Kentish, Enhancing gas permeability in mixed matrix membranes through tuning the nanoparticle properties, *J. Membr. Sci.* 482 (2015) 49–55.
- [39] L. Cipelletti, J.-P. Biron, M. Martin, H. Cottet, Polydispersity analysis of taylor dispersion data: the cumulant method, *Anal. Chem.* 86 (2014) 6471–6478.
- [40] Q. Song, S.K. Nataraj, M.V. Roussanova, J.C. Tan, D.J. Hughes, W. Li, P. Bourgoin, M.A. Alam, A.K. Cheetham, S.A. Al-Muhtaseb, E. Sivaniah, Zeolitic imidazolate framework (ZIF-8) based polymer nanocomposite membranes for gas separation, *Energy Environ. Sci.* 5 (2012) 8359–8369.
- [41] S. Shahid, K. Nijmeijer, Performance and plasticization behavior of polymer–MOF membranes for gas separation at elevated pressures, *J. Membr. Sci.* 470 (2014) 166–177.
- [42] N.A.H.M. Nordin, A.F. Ismail, A. Mustafa, R.S. Murali, T. Matsuura, The impact of ZIF-8 particle size and heat treatment on CO₂/CH₄ separation using asymmetric mixed matrix membrane, *RSC Adv.* 4 (2014) 52530–52541.
- [43] K.S. Park, Z. Ni, A.P. Côté, J.Y. Choi, R. Huang, F.J. Uribe-Romo, H.K. Chae, M. O'Keeffe, O.M. Yaghi, Exceptional chemical and thermal stability of zeolitic imidazolate frameworks, *Proc. Natl. Acad. Sci.* 103 (2006) 10186–10191.
- [44] S. Wang, Y. Liu, S. Huang, H. Wu, Y. Li, Z. Tian, Z. Jiang, Pebax–PEG–MWCNT hybrid membranes with enhanced CO₂ capture properties, *J. Membr. Sci.* 460 (2014) 62–70.
- [45] A. Car, C. Stropnik, W. Yave, K.-V. Peinemann, PEG modified poly(amide-b-ethylene oxide) membranes for CO₂ separation, *J. Membr. Sci.* 307 (2008) 88–95.
- [46] A. Ghadimi, M. Amirilargani, T. Mohammadi, N. Kasiri, B. Sadatnia, Preparation of alloyed poly(ether block amide)/poly(ethylene glycol diacrylate) membranes for separation of CO₂/H₂ (syngas application), *J. Membr. Sci.* 458 (2014) 14–26.
- [47] J.H. Kim, Y.M. Lee, Gas permeation properties of poly(amide-6-b-ethylene oxide)–silica hybrid membranes, *J. Membr. Sci.* 193 (2001) 209–225.
- [48] E.M. Mahdi, J.-C. Tan, Mixed-matrix membranes of zeolitic imidazolate framework (ZIF-8)/Matrimid nanocomposite: thermo-mechanical stability and viscoelasticity underpinning membrane separation performance, *J. Membr. Sci.* 498 (2016) 276–290.
- [49] E.M. Mahdi, J.-C. Tan, Dynamic molecular interactions between polyurethane and ZIF-8 in a polymer-MOF nanocomposite: microstructural, thermo-mechanical and viscoelastic effects, *Polymer* 97 (2016) 31–43.
- [50] J. Shen, G. Liu, K. Huang, Q. Li, K. Guan, Y. Li, W. Jin, UiO-66-polyether block amide mixed matrix membranes for CO₂ separation, *J. Membr. Sci.* 513 (2016) 155–165.
- [51] H. Rabiee, A. Ghadimi, T. Mohammadi, Gas transport properties of reverse-selective poly(ether-b-amide6)/[Emim][BF₄] gel membranes for CO₂/light gases separation, *J. Membr. Sci.* 476 (2015) 286–302.
- [52] V.I. Bondar, B.D. Freeman, I. Pinnau, Gas transport properties of poly(ether-b-amide) segmented block copolymers, *J. Polym. Sci. Part B: Polym. Phys.* 38 (2000) 2051–2062.
- [53] D. Fairen-Jimenez, S.A. Moggach, M.T. Wharmby, P.A. Wright, S. Parsons, T. Düren, Opening the gate: framework flexibility in ZIF-8 explored by experiments and simulations, *J. Am. Chem. Soc.* 133 (2011) 8900–8902.
- [54] V. Nafisi, M.-B. Hägg, Development of dual layer of ZIF-8/PEBAX-2533 mixed matrix membrane for CO₂ capture, *J. Membr. Sci.* 459 (2014) 244–255.
- [55] A. Bos, I.G.M. Pünt, M. Wessling, H. Strathmann, CO₂-induced plasticization phenomena in glassy polymers, *J. Membr. Sci.* 155 (1999) 67–78.
- [56] A.F. Ismail, W. Lorna, Penetrant-induced plasticization phenomenon in glassy polymers for gas separation membrane, *Sep. Purif. Technol.* 27 (2002) 173–194.
- [57] E.S. Sanders, Penetrant-induced plasticization and gas permeation in glassy polymers, *J. Membr. Sci.* 37 (1988) 63–80.
- [58] J.A. Thompson, J.T. Vaughn, N.A. Brunelli, W.J. Koros, C.W. Jones, S. Nair, Mixed-linker zeolitic imidazolate framework mixed-matrix membranes for aggressive CO₂ separation from natural gas, *Microporous Mesoporous Mater.* 192 (2014) 43–51.
- [59] C.A. Scholes, G.W. Stevens, S.E. Kentish, The effect of hydrogen sulfide, carbon monoxide and water on the performance of a PDMS membrane in carbon dioxide/nitrogen separation, *J. Membr. Sci.* 350 (2010) 189–199.
- [60] S. Chen, K. Yao, F.E.H. Tay, L.L.S. Chew, Comparative investigation of the structure and properties of ferroelectric poly(vinylidene fluoride) and poly(vinylidene fluoride–trifluoroethylene) thin films crystallized on substrates, *J. Appl. Polym. Sci.* 116 (2010) 3331–3337.
- [61] D.F. Sanders, Z.P. Smith, R. Guo, L.M. Robeson, J.E. McGrath, D.R. Paul, B.D. Freeman, Energy-efficient polymeric gas separation membranes for a sustainable future: a review, *Polymer* 54 (2013) 4729–4761.
- [62] P. Bernardo, E. Drioli, G. Golemme, Membrane gas separation: a review/state of the art, *Ind. Eng. Chem. Res.* 48 (2009) 4638–4663.
- [63] S. Adhikari, S. Fernando, Hydrogen membrane separation techniques, *Ind. Eng. Chem. Res.* 45 (2006) 875–881.
- [64] J.M.P. Scofield, P.A. Gurr, J. Kim, Q. Fu, S.E. Kentish, G.G. Qiao, Development of novel fluorinated additives for high performance CO₂ separation thin-film composite membranes, *J. Membr. Sci.* 499 (2016) 191–200.
- [65] J.M.P. Scofield, P.A. Gurr, J. Kim, Q. Fu, A. Halim, S.E. Kentish, G.G. Qiao, High-performance thin film composite membranes with well-defined poly(dimethylsiloxane)-b-poly(ethylene glycol) copolymer additives for CO₂ separation, *J. Polym. Sci. Part A: Polym. Chem.* 53 (2015) 1500–1511.
- [66] K. Takada, H. Matsuya, T. Masuda, T. Higashimura, Gas permeability of poly-acetylenes carrying substituents, *J. Appl. Polym. Sci.* 30 (1985) 1605–1616.

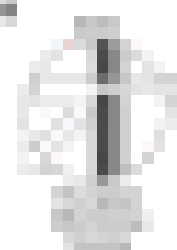
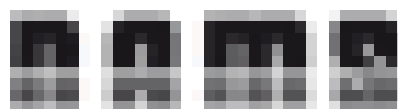


ISSN 0368-2031 (print) ISSN 0950-4230 (online)
CODEN JMSEDD

journal of MEMBRANE SCIENCE



The Journal is endorsed by the American, European, and
North American Membrane Societies



MEMBRANE SOCIETY OF AMERICA
MEMBERSHIP



ScienceDirect

Fuzzy Sets and Systems

Supports *open access*

7.0

CiteScore

3.343

Impact Factor

[Submit your article](#)

[Guide for authors](#)

Menu

[Search in this journal](#)

About the journal

[Aims and scope](#)

[Editorial board](#)

[Abstracting and indexing](#)

Co Editors-in-Chief

I. Couso

University of Oviedo, Oviedo, Spain

[Email this editor](#)



B. De Baets

Ghent University Department of Data Analysis and Mathematical Modelling, St. Pietersnieuwstraat 33, 9000, Ghent,, Belgium

[Email this editor](#)



L. Godo

Artificial Intelligence Research Institute, Campus UAB s/n, 08193, Bellaterra, Spain

[Email this editor](#)

Former Editors-in-Chief

H.J. Zimmermann

H. Prade

E. Hüllermeier

D. Dubois

Honorary Editor

FEEDBACK

L.A. Zadeh†

University of California Berkeley Division of Computer Science, CA 94720-1776, Berkeley, California, United States of America

Advisory Editors

J.C. Bezdek

The University of Melbourne Department of Computing and Information Systems, 111 Barry Street - Building 168, Melbourne, 3010, Australia

B. Bouchon-Meunier

Sorbonne University, 75005, Paris, France

U. Höhle

University of Wuppertal, Pauluskirchstraße 7, 42285, Wuppertal, Germany

J. Kacprzyk

Polish Academy of Sciences, 00-901, Warszawa, Poland

E.P. Klement

Johannes Kepler University Linz, Altenbergerstr. 69, 4040, Linz, Austria

R. Kruse

Otto-von-Guericke-University Magdeburg Faculty of Computer Science, Postfach 4120, Magdeburg, Germany

Y.-M. Liu

Sichuan University, Chengdu, 610065, Chengdu, Sichuan, China

H.T. Nguyen

New Mexico State University, 88003-8006, Las Cruces, New Mexico, United States of America

D. Ralescu

University of Cincinnati, 45221, Cincinnati, Ohio, United States of America

E.H. Ruspini

M. Sugeno

Doshisha University Faculty of Culture and Information Science, 1-3 Miyakodani Tatara, Kyonatabe, 610-0394, Kyoto, Japan

E. Trillas

University of Oviedo, Oviedo, Spain

J.L. Verdegay

Int. Artificial, Depto. de Ciencias de la Computacion, Universidad de Granada,Codigo Correspondencia Para Organismos Oficiales,, 18071, Granada, Spain

R.R. Yager

Iona College Machine Intelligence Institute, New Rochelle, 10801, New Rochelle, New York, United States of America

Area Editors

P. Angelov

Lancaster, United Kingdom

Hybrid Systems

G. Beliakov

Burwood, Victoria, Australia

Aggregation Operations

R. Belohlavek

Olomouc, Czechia

Algebra

M. Bernal

Ciudad Obregon, Mexico

Control Engineering

I. Bloch

Paris, France

Image Processing

J.P. Carvalho

Lisbon, Portugal

Fuzzy systems

L. Coroianu

Oradea, Romania

Fuzzy intervals

I. Couso

Oviedo, Spain

Fuzzy sets and Possibility theory

[Email this editor](#) ↗

L.C. De Barros

Campinas, São Paulo, Brazil

Differential equations

S. Díaz Vázquez

Oviedo, Spain

Preference modeling

T Flaminio

Bellaterra, Spain

Uncertainty and game theory in many-valued structures

J.L. García-Lapresta

Valladolid, Spain

Preference Modeling & Decision Analysis

T-M. Guerra

Valenciennes, France

Control Engineering

J. Gutierrez Garcia

Bilbao, Spain

Topology & Category Theory

M. Inuiguchi

Toyonaka, Japan

Optimisation & Mathematical Programming

FEEDBACK 

B. Jayaram
Kandi, India
Aggregation operations

R. Mesiar
Bratislava, Slovakia
Aggregation Functions

C. Noguera, PhD
Praha, Czechia

A.M. Ojeda-Aciego
Malaga, Spain
Fuzzy Formal concept analysis and fuzzy logic programming

E. Pap
Novi Sad, Serbia
Measure Theory

M. Reformat
Edmonton, Alberta, Canada
Research Interests, develop methods and techniques for modeling data and knowledge, as well as design systems which possess abilities to imitate different aspects of human behavior

A. Rico
Lyon, France
Aggregation operations

D. Sánchez
Granada, Spain
Data Mining and Learning

M. Sato-Ilic
Tsukuba, Japan
Clustering

S. Schockaert, PhD
Cardiff, United Kingdom
Logics and Artificial Intelligence

L. Stefanini
Urbino, Italy
Fuzzy Intervals

M. Stepnicka
Ostrava, Czechia
Fuzzy Rule-Based Systems

T. Sudkamp
Dayton, Ohio, United States of America
Engineering Applications

B. Vantaggi
Roma, Italy
Probability and statistics

T. Vetterlein
Linz, Austria
Algebraic Aspects of Fuzzy Sets

S. Zadrozny
Warszawa, Poland
Information Systems

D. Zhang
Chengdu, Sichuan, China
Topology

Book Review Editor

A. Gegov
Portsmouth, United Kingdom
[Email this editor](#) ↗

Editorial Board

S. Aguzzoli
Milan, Italy

T. Allahviranloo
İstanbul, Turkey

M. Baczynski
Katowice, Poland

A. I. Ban
Oradea, Romania

M. Banerjee
Kanpur, India

T. Bilgic
İstanbul, Turkey

P. Bonissone
Schenectady, New York, United States of America

B. Bouchon-Meunier
Paris, France

A. Bronevich
Moscow, Russian Federation

H. Bustince
Pamplona, Spain

Y.-K. Cai
Beijing, China

C. Carlsson

Åbo, Finland

G. Chen
Beijing, China

P. Cintula
Praha, Czechia

M. Ćirić
Nis, Serbia

D. Ciucci
Milano, Italy

C. Cornelis
Gent, Belgium

J.M. Costa Sousa
Lisbon, Portugal

P. D'Urso, PhD
Roma, Italy

G. De Tré
Gent, Belgium

M. Demirci
Antalya, Turkey

T. Denoeux, PhD
Compiègne, France

A. Di Nola
Fisciano, Italy

F. Durante
Lecce, Italy

E. Esmi
Campinas, São Paulo, Brazil

M Ferraro
Roma, Italy

H. Frigui
Louisville, Kentucky, United States of America

S. Galichet
Annecy, France

B. Gerla
Varese, Italy

M.A. Gil
Oviedo, Spain

FEEDBACK 

Z. Gong

Lanzhou, Gansu, China

M. Grabisch

Paris, France

S. Greco

Catania, Italy

M. Hanss

Stuttgart, Germany

F. H. Herrera

Granada, Spain

E. Herrera-Viedma

Granada, Spain

U. Höhle

Wuppertal, Germany

M. Holcapek

Ostrava, Czechia

J. Kacprzyk

Warszawa, Poland

M. Kalina

Bratislava, Slovakia

A. Kasperski

Wroclaw, Poland

U Kaymak

Eindhoven University of Technology, Eindhoven, Netherlands

J.M. Keller

Columbia, Missouri, United States of America

A. Khastan

Zanjan, Iran

F. Klawonn

Wolfenbüttel, Germany

E.P. Klement

Linz, Austria

T. Kóczy, Ph.D., D.Sc.

Budapest, Hungary

T. Kubiak

Poznan, Poland

H. Lai

Qingyang, Sichuan, China

FEEDBACK 

H.L. Larsen
Esbjerg, Denmark

J. Lawry
Bristol, United Kingdom

Z. Lendek
Cluj-Napoca, Romania

C.-J. Liau
Taipei, Taiwan

W.A. Lodwick
Denver, Colorado, United States of America

V. Lupulescu
Târgu Jiu, Romania

T. Marchant
Gent, Belgium

J.-L. Marichal
Esch-Sur-Alzette, Luxembourg

R. A. Marques Pereira
Trento, Italy

C. Marsala
Paris, France

T. Martin
Bristol, United Kingdom

S. Massanet
Palma de Mallorca, Spain

S. Miyamoto
Ibaraki, Japan

J. Montero
Madrid, Spain

S. Montes Rodríguez
Oviedo, Spain

J.N. Mordeson
Omaha, Nebraska, United States of America

T. Murofushi
Yokohama, Japan

S. Muzzioli
Modena, Italy

M. Navara
Praha, Czechia

FEEDBACK 

H.T. Nguyen

Las Cruces, New Mexico, United States of America

J.J. Nieto

Santiago de Compostela, Spain

V. Nývák

Ostrava, Czechia

N.R. Pal

Kolkata, India

S.K. Pal

Kolkata, India

G. Pasi

Milan, Italy

W. Pedrycz

Edmonton, Alberta, Canada

K. Peeva

Sofia, Bulgaria

I. Perfilieva

Ostrava, Czechia

F.E. Petry

Stennis Space Center, Mississippi, United States of America

O. Pivert

Lannion Cedex, France

H. Prade

Toulouse, France

D. Ralescu

Cincinnati, Ohio, United States of America

J. Ramik

Karvina, Czechia

A. B. Ramos-Guajardo

Oviedo, Spain

R. Rodriguez-Lopez

Santiago de Compostela, Spain

R. O. Rodriguez

Buenos Aires, Argentina

E.H. Ruspini

S. Sessa

Naples, Italy

FEEDBACK 

Q. Shen

Aberystwyth, United Kingdom

R. Słowiński, PhD, Full Professor

Poznan, Poland

A. Sostaks

Rīga, Latvia

U. Straccia

Pisa, Italy

O. Strauss

Montpellier, France

A. Stupňanová

Bratislava, Slovakia

P. Sussner

Campinas, São Paulo, Brazil

A. Tepavcevic

Novi Sad, Serbia

V. Torra

Bellaterra, Spain

W. Trutschnig

Mieres, Spain

R.R. Yager

New Rochelle, New York, United States of America

H. Ying

Detroit, Michigan, United States of America

J. Yoneyama

Shibuya-Ku, Japan

All members of the Editorial Board have identified their affiliated institutions or organizations, along with the corresponding country or geographic region. Elsevier remains neutral with regard to any jurisdictional claims.

ISSN: 0165-0114

Copyright © 2022 Elsevier B.V. All rights reserved



Copyright © 2022 Elsevier B.V. or its licensors or contributors.
ScienceDirect® is a registered trademark of Elsevier B.V.

RELX™

FEEDBACK



ScienceDirect

Journal of Membrane Science

Supports open access

13.5

CiteScore

8.742

Impact Factor

[Submit your article](#)

[Guide for authors](#)

Menu

Search in this journal

Volume 524

Pages 1-772 (15 February 2017)

[Download full issue](#)

[Previous vol/issue](#)

[Next vol/issue](#)

Receive an update when the latest issues in this journal are published

[Sign in to set up alerts](#)

[Full text access](#)

[Inside front cover](#)

[Page IFC](#)

[Download PDF](#)

Reviews

[Review article](#) [Full text access](#)

Molecular simulations of polyamide membrane materials used in desalination and water reuse applications: Recent developments and future prospects

Harry F. Ridgway, John Orbell, Stephen Gray

Pages 436-448

[Download PDF](#) [Article preview](#)

[Review article](#) [Full text access](#)

Progress and perspectives for synthesis of sustainable antifouling composite membranes containing *in situ* generated nanoparticles

Xin Li, Arcadio Sotto, Jiansheng Li, Bart Van der Bruggen

Pages 502-528

FEEDBACK

[Download PDF](#) Article preview 

Original Research Papers

Research article Full text access

Fabrication of high silicalite-1 content filled PDMS thin composite pervaporation membrane for the separation of ethanol from aqueous solutions

Haoli Zhou, Jinqiang Zhang, Yinhua Wan, Wanqin Jin

Pages 1-11

[Download PDF](#) Article preview 

Research article Full text access

Room-temperature ionic liquids modified zeolite SSZ-13 membranes for CO₂/CH₄ separation

Bo Liu, Rongfei Zhou, Na Bu, Qing Wang, ... Kita Hidetoshi

Pages 12-19

[Download PDF](#) Article preview 

Research article Full text access

Investigation of single-pass tangential flow filtration (SPTFF) as an inline concentration step for cell culture harvest

Abhiram Arunkumar, Nripen Singh, Michael Peck, Michael C. Borys, Zheng Jian Li

Pages 20-32

[Download PDF](#) Article preview 

Research article Full text access

Molecular interaction between acidic sPPSU and basic HPEI polymers and its effects on membrane formation for ultrafiltration

Lin Luo, Tai-Shung Chung, Martin Weber, Claudia Staudt, Christian Maletzko

Pages 33-42

[Download PDF](#) Article preview 

Research article Full text access

Hydrophilic fouling-resistant GO-ZnO/PES membranes for wastewater reclamation

O.T. Mahlangu, R. Nackaerts, J.M. Thwala, B.B. Mamba, A.R.D. Verliefde

Pages 43-55

[Download PDF](#) Article preview 

Research article Full text access

Oxygen permeation and stability of CaTi_{0.73}Fe_{0.18}Mg_{0.09}O_{3-δ} oxygen-transport membrane

Maria Balaguer, Sonia Escolástico, Jose M. Serra

Pages 56-63

[Download PDF](#) Article preview 

Research article Full text access

Pore size tuning of sol-gel-derived triethoxysilane (TRIES) membranes for gas separation

Masakoto Kanezashi, Rui Matsugasako, Hiromasa Tawarayama, Hiroki Nagasawa, Toshinori Tsuru

Pages 64-72

FEEDBACK 

[Download PDF](#) Article preview 

Research article *Open access*

High-capacity open bore membrane chromatography column based on micro-packed ceramic hollow fibres

Melanie Lee, Bo Wang, Kang Li

Pages 73-78

[Download PDF](#) Article preview 

Research article Full text access

Development of enzyme-loaded PVA microspheres by membrane emulsification

Emma Piacentini, Mengying Yan, Lidietta Giorno

Pages 79-86

[Download PDF](#) Article preview 

Research article Full text access

Effects of membrane structure and operational variables on membrane distillation performance

Vasiliki Karanikola, Andrea F. Corral, Hua Jiang, A. Eduardo Sáez, ... Robert G. Arnold

Pages 87-96

[Download PDF](#) Article preview 

Research article Full text access

Tuning water content in polymer dopes to boost the performance of outer-selective thin-film composite (TFC) hollow fiber membranes for osmotic power generation

Zhen Lei Cheng, Xue Li, Yingnan Feng, Chun Feng Wan, Tai-Shung Chung

Pages 97-107


[Download PDF](#) Article preview 

Research article Full text access

Permeate flux prediction in the ultrafiltration of fruit juices by ARIMA models

René Ruby-Figueroa, Jorge Saavedra, Natalia Bahamonde, Alfredo Cassano

Pages 108-116

[Download PDF](#) Article preview 

Research article Full text access

Thin SAPO-34 membranes synthesized in stainless steel autoclaves for N₂/CH₄ separation

Zhaowang Zong, Moises A. Carreon

Pages 117-123

[Download PDF](#) Article preview 

Research article Full text access

Effects of sodium ions on the separation performance of pure-silica MFI zeolite membranes

Chenchen Xu, Xiaofei Lu, Zhengbao Wang

Pages 124-131

[Download PDF](#) Article preview 

Research article Full text access

Separation performance of novel vinyltriethoxysilane (VTES)-g-silicalite-1/PDMS/PAN thin-film co

FEEDBACK 

membrane in the recovery of bioethanol from fermentation broths by pervaporation

Shouliang Yi, Yinhua Wan

Pages 132-140

[Download PDF](#) Article preview 

Research article Full text access

One-step preparation of high-performance bilayer α -alumina ultrafiltration membranes via co-sintering process

Dong Zou, Minghui Qiu, Xianfu Chen, Yiqun Fan

Pages 141-150

[Download PDF](#) Article preview 

Research article Open access

Membrane distillation against a pressure difference

L. Keulen, L.V. van der Ham, N.J.M. Kuipers, J.H. Hanemaaijer, ... S. Kjelstrup

Pages 151-162

[Download PDF](#) Article preview 

Research article Full text access

Rational design and synthesis of molecular-sieving, photocatalytic, hollow fiber membranes for advanced water treatment applications

David K. Wang, Muthia Elma, Julius Motuzas, Wen-Che Hou, ... Xiwang Zhang

Pages 163-173

[Download PDF](#) Article preview 

Research article Full text access

Cellulose nanofiber intermediary to fabricate highly-permeable ultrathin nanofiltration membranes for fast water purification

Faizal Soyekwo, Qiugen Zhang, Runsheng Gao, Yan Qu, ... Qinglin Liu

Pages 174-185

[Download PDF](#) Article preview 

Research article Full text access

Mathematical modeling of CO₂ absorption into novel reactive DEAB solution in hollow fiber membrane contactors; kinetic and mass transfer investigation

Majid Saidi

Pages 186-196

[Download PDF](#) Article preview 

Research article Full text access

"Butterfly Effect" from finite dope chemical composition variations on the water/oil separation capabilities of super rough polyvinylidene difluoride (PVDF) porous membranes

Qing Yang, Ailin Gao, Lixin Xue

Pages 197-204

[Download PDF](#) Article preview 

Research article Full text access

Selective transport and simultaneous separation of Cu(II), Zn(II) and Mg(II) using a dual polymer inclusion membrane

FEEDBACK 

membrane system

Duo Wang, Jiugang Hu, Dabiao Liu, Qiyuan Chen, Jie Li

Pages 205-213

[Download PDF](#) [Article preview](#) 

Research article [Full text access](#)

A loose nano-filtration membrane prepared by coating HPAN UF membrane with modified PEI for dye reuse and desalination

Shuang Zhao, Zhan Wang

Pages 214-224

[Download PDF](#) [Article preview](#) 

Research article [Full text access](#)

Three-dimensional reconstruction of bioactive membranes and pore-scale simulation of enzymatic reactions: The case of lactose hydrolysis

N. Bali, A.J. Petsi, E.D. Skouras, V.N. Burganos

Pages 225-234

[Download PDF](#) [Article preview](#) 

Research article [Full text access](#)

Structures and antifouling properties of polyvinyl chloride/poly(methyl methacrylate)-graft-poly(ethylene glycol) blend membranes formed in different coagulation media

Li-Feng Fang, Bao-Ku Zhu, Li-Ping Zhu, Hideto Matsuyama, Shuaifei Zhao

Pages 235-244

[Download PDF](#) [Article preview](#) 

Research article [Full text access](#)

Full-scale direct contact membrane distillation (DCMD) model including membrane compaction effects

I. Hitsov, L. Eykens, W. De Schepper, K. De Sitter, ... I. Nopens

Pages 245-256

[Download PDF](#) [Article preview](#) 

Research article [Full text access](#)

Kinetics of poly(ethylene glycol) extraction into water from plasticized disulfonated poly(arylene ether sulfone) desalination membranes prepared by solvent-free melt processing

Hee Jeung Oh, James E. McGrath, Donald R. Paul

Pages 257-265

[Download PDF](#) [Article preview](#) 

Research article [Full text access](#)

Improved operational stability of Pebax-based gas separation membranes with ZIF-8: A comparative study of flat sheet and composite hollow fibre membranes

Putu Doddy Sutrisna, Jingwei Hou, Hongyu Li, Yatao Zhang, Vicki Chen

Pages 266-279

[Download PDF](#) [Article preview](#) 

Research article [Full text access](#)

FEEDBACK 

Energy efficiency enhancement of electromembrane desalination systems by local flow redistribution optimized for the asymmetry of cation/anion diffusivity

Bumjoo Kim, Siwon Choi, Van Sang Pham, Rhokyun Kwak, Jongyoon Han

Pages 280-287

[Download PDF](#) [Article preview](#) 

Research article [Full text access](#)

Fouling control using critical, threshold and limiting fluxes concepts for cross-flow NF of a complex matrix: Membrane BioReactor effluent

Yandi Lan, Karine Groenen-Serrano, Clémence Coetsier, Christel Causserand

Pages 288-298

[Download PDF](#) [Article preview](#) 

Research article [Full text access](#)

Analysis of the onset of calcium sulfate scaling on RO membranes

Marina Shmulevsky, Xianhui Li, Hilla Shemer, David Hasson, Raphael Semiat

Pages 299-304

[Download PDF](#) [Article preview](#) 

Research article [Full text access](#)

Separation and concentration of milk proteins with a submerged membrane vibrational system

Milton Chai, Yun Ye, Vicki Chen

Pages 305-314

[Download PDF](#) [Article preview](#) 

Research article [Full text access](#)

Enhanced separator wettability by LiTFSI and its application for lithium metal batteries

Yong Xie, Hongfa Xiang, Pengcheng Shi, Jipeng Guo, Haihui Wang

Pages 315-320

[Download PDF](#) [Article preview](#) 

Research article [Full text access](#)

Experimental investigation and modeling through using the solution-diffusion concept of pervaporation dehydration of ethanol and isopropanol by ceramic membranes HybSi

Alexander V. Klinov, Roald R. Akberov, Azat R. Fazlyev, Mansur I. Farakhov

Pages 321-333

[Download PDF](#) [Article preview](#) 

Research article [Full text access](#)

Simulation of the effect of the porous support on flux through an asymmetric oxygen transport membrane

U. Unije, R. Mücke, P. Niehoff, S. Baumann, ... O. Guillon

Pages 334-343

[Download PDF](#) [Article preview](#) 

Research article [Full text access](#)

Sulfonated multiwall carbon nanotubes assisted thin-film nanocomposite membrane with enhanced water flux and anti-fouling property

FEEDBACK 

Junfeng Zheng, Meng Li, Kai Yu, Jiahui Hu, ... Lianjun Wang

Pages 344-353

[Download PDF](#) [Article preview](#) 

Research article [Full text access](#)

V-Cr-Cu dual-phase alloy membranes for hydrogen separation: An excellent combination of ductility, hydrogen permeability and embrittlement resistance

Xinzhong Li, Feifei Huang, Dongmei Liu, Xiao Liang, ... Hengzhi Fu

Pages 354-361

[Download PDF](#) [Article preview](#) 

Research article [Full text access](#)

An integrative modeling and experimental study on the ionic resistance of ion-exchange membranes

Bopeng Zhang, Jin Gi Hong, Shihua Xie, Shuman Xia, Yongsheng Chen

Pages 362-369

[Download PDF](#) [Article preview](#) 

Research article [Full text access](#)

Improving the water dissociation efficiency in a bipolar membrane with amino-functionalized MIL-101

Qiuyue Wang, Bin Wu, Chenxiao Jiang, Yaoming Wang, Tongwen Xu

Pages 370-376

[Download PDF](#) [Article preview](#) 

Research article [Full text access](#)

Microparticles for cell encapsulation and colonic delivery produced by membrane emulsification

S. Morelli, R.G. Holdich, M.M. Dragosavac

Pages 377-388

[Download PDF](#) [Article preview](#) 

Research article [Full text access](#)

Functional surface modification of PVDF membrane for chemical pulse cleaning

Zhong Ma, Xiaolong Lu, Chunrui Wu, Qijun Gao, ... Zhiyu Liu

Pages 389-399

[Download PDF](#) [Article preview](#) 

Research article [Full text access](#)

Numerical simulation of ionic transport processes through bilayer ion-exchange membranes in reverse electro dialysis stacks

A.A. Moya

Pages 400-408

[Download PDF](#) [Article preview](#) 

Research article [Full text access](#)

A catechol-based biomimetic strategy combined with surface mineralization to enhance hydrophilicity and anti-fouling property of PTFE flat membrane

Sikuai Xue, Chengcai Li, Jiuming Li, Hailin Zhu, Yuhai Guo

Pages 409-418

FEEDBACK 

[Download PDF](#) [Article preview](#) 

Research article [Full text access](#)

Polymer electrolyte membranes prepared by pre-irradiation induced graft copolymerization on ETFE for vanadium redox flow battery applications

Xin Li, Antonio R. dos Santos, Marco Drache, Xi Ke, ... Sabine Beuermann

Pages 419-427

[Download PDF](#) [Article preview](#) 

Research article [Full text access](#)

Ultra-thin MFI membranes for olefin/nitrogen separation

Liang Yu, Mattias Grahn, Pengcheng Ye, Jonas Hedlund

Pages 428-435

[Download PDF](#) [Article preview](#) 

Research article [Full text access](#)

Bio-based membranes for ethyl tert-butyl ether (ETBE) bio-fuel purification by pervaporation

Faten Hassan Hassan Abdellatif, Jérôme Babin, Carole Arnal-Herault, Cécile Nouvel, ... Anne Jonquieres

Pages 449-459

[Download PDF](#) [Article preview](#) 

Research article [Full text access](#)

Application of coagulation-UF hybrid process for shale gas fracturing flowback water recycling: Performance and fouling analysis

Fan-xin Kong, Jin-fu Chen, He-ming Wang, Xiao-ning Liu, ... Yuefeng F. Xie

Pages 460-469

[Download PDF](#) [Article preview](#) 

Research article [Full text access](#)

Production of very-high purity succinic acid from fermentation broth using microfiltration and nanofiltration-assisted crystallization

Nguyen Thi Huong Thuy, Apichat Boontawan

Pages 470-481

[Download PDF](#) [Article preview](#) 

Research article [Full text access](#)

Electrochemical acidification of Kraft black liquor: Impacts of pulsed electric field application on bipolar membrane colloidal fouling and process intensification

Maryam Haddad, Laurent Bazinet, Oumarou Savadogo, Jean Paris

Pages 482-492

[Download PDF](#) [Article preview](#) 

Research article [Full text access](#)

Fouling in direct contact membrane distillation of produced water from unconventional gas extraction

Omkar R. Lokare, Sakineh Tavakkoli, Shardul Wadekar, Vikas Khanna, Radisav D. Vidic

Pages 493-501

[Download PDF](#) [Article preview](#) 

FEEDBACK 

Research article Full text access

The tolerance of a thin-film composite polyamide reverse osmosis membrane to hydrogen peroxide exposure

Ran Ling, Ling Yu, Thi Phuong Thuy Pham, Jiahui Shao, ... Martin Reinhard

Pages 529-536

[Download PDF](#) Article preview 

Research article Full text access

Hydrophilization of polysulfone hollow fiber membranes via addition of polyvinylpyrrolidone to the bore fluid

Alexandr V. Bilydukevich, Tatiana V. Plisko, Alena S. Liubimova, Vladimir V. Volkov, Vadim V. Usosky

Pages 537-549

[Download PDF](#) Article preview 

Research article Full text access

Polymer electrolyte membrane with heterocyclic terminated poly(ethylene glycol) brushes: An approach to decorate proton conductive species on membrane surface

Adisak Pokprasert, Suwabun Chirachanchai

Pages 550-556

[Download PDF](#) Article preview 

Research article Full text access

Preparation of porous diffusion dialysis membranes by functionalization of polysulfone for acid recovery

Xiaocheng Lin, Seungju Kim, De Ming Zhu, Ezzatollah Shamsaei, ... Huanting Wang

Pages 557-564

[Download PDF](#) Article preview 

Research article Full text access

Membrane distillation for wastewater reverse osmosis concentrate treatment with water reuse potential

Gayathri Naidu, Sanghyun Jeong, Youngkwon Choi, Saravanamuthu Vigneswaran

Pages 565-575

[Download PDF](#) Article preview 

Research article Full text access

Enhancing water vapor permeability in mixed matrix polypropylene membranes through carbon nanotubes dispersion

G. Bounos, K.S. Andrikopoulos, H. Moschopoulou, G.Ch. Lainioti, ... G.A. Voyiatzis

Pages 576-584

[Download PDF](#) Article preview 

Research article Full text access

Pore morphology and temperature dependence of gas transport properties of silica membranes derived from oxidative thermolysis of polydimethylsiloxane

Jason Adams, Neha Bighane, William J. Koros

Pages 585-595

[Download PDF](#) Article preview 

Research article Full text access

Robust CO₂ and H₂ resistant triple-layered (Ag-YSZ)/YSZ/(La_{0.8}Sr_{0.2}MnO_{3-δ}-YSZ) hollow fiber membrane

FEEDBACK 

short-circuit for oxygen permeation

Xiuxia Meng, Jaka Sunarso, Yun Jin, Xiuxiu Bi, ... Shaomin Liu

Pages 596-603

[Download PDF](#) [Article preview](#) 

Research article [Full text access](#)

Dynamic membrane filtration using powdered iron oxide for SWRO pre-treatment during red tide event

Byeong-Cheol Kim, Jong-Woo Nam, Ki-Hoon Kang

Pages 604-611

[Download PDF](#) [Article preview](#) 

Research article [Full text access](#)

Developing nanofiltration membrane based on microporous poly(tetrafluoroethylene) substrates by bi-stretching process

Hongyan Tang, Jun He, Liting Hao, Feng Wang, ... Yuhai Guo

Pages 612-622

[Download PDF](#) [Article preview](#) 

Research article [Full text access](#)

ECTFE hybrid porous membrane with hierarchical micro/nano-structural surface for efficient oil/water separation

Jian Pan, Changfa Xiao, Qinglin Huang, Hailiang Liu, Tai Zhang

Pages 623-630

[Download PDF](#) [Article preview](#) 

Research article [Full text access](#)

Combinatorial screening of Pd-Ag-Ni membranes for hydrogen separation

Fatih Pişkin, Tayfur Öztürk

Pages 631-636

[Download PDF](#) [Article preview](#) 

Research article [Full text access](#)

Extending the uppermost pore diameter measurable via Evaporimetry

Farhad Zamani, Praveena Jayaraman, Ebrahim Akhondi, William B. Krantz, ... Jia Wei Chew

Pages 637-643

[Download PDF](#) [Article preview](#) 

Research article [Full text access](#)

Atmospheric-pressure plasma-enhanced chemical vapor deposition of microporous silica membranes for gas separation

Hiroki Nagasawa, Yuta Yamamoto, Nobukazu Tsuda, Masakoto Kanezashi, ... Toshinori Tsuru

Pages 644-651

[Download PDF](#) [Article preview](#) 

Research article [Full text access](#)

Ionic liquid-modified Pebax® 1657 membrane filled by ZIF-8 particles for separation of CO₂ from CH₄, N₂ and H₂

Abolfazl Jomekian, Bahamin Bazooyar, Reza Mosayebi Behbahani, Toraj Mohammadi, Ali Kargari

Pages 652-662

FEEDBACK 

[Download PDF](#) [Article preview](#) 

Research article [Full text access](#)

Sulfonated reduced graphene oxide as a conductive layer in sulfonated poly(ether ether ketone) nanocomposite membranes

Xiang Qiu, Tiandu Dong, Mitsuru Ueda, Xuan Zhang, Lianjun Wang
Pages 663-672

[Download PDF](#) [Article preview](#) 

Research article [Full text access](#)

Spatially-resolved *in-situ* quantification of biofouling using optical coherence tomography (OCT) and 3D image analysis in a spacer filled channel

Luca Fortunato, Szilárd Bucs, Rodrigo Valladares Linares, Corrado Cali, ... TorOve Leiknes
Pages 673-681

[Download PDF](#) [Article preview](#) 

Research article [Full text access](#)

Liquid filtration of nanoparticles through track-etched membrane filters under unfavorable and different ionic strength conditions: Experiments and modeling

Handol Lee, Doris Segets, Sebastian Süß, Wolfgang Peukert, ... David Y.H. Pui
Pages 682-690

[Download PDF](#) [Article preview](#) 

Research article [Full text access](#)

In situ MRI of alginate fouling and flow in ceramic hollow fiber membranes

F. Arndt, S. Schuhmann, G. Guthausen, S. Schütz, H. Nirschl
Pages 691-699

[Download PDF](#) [Article preview](#) 

Research article [Full text access](#)

SiO₂-ZrO₂ nanofiltration membranes of different Si/Zr molar ratios: Stability in hot water and acid/alkaline solutions

Waravut Puthai, Masakoto Kanezashi, Hiroki Nagasawa, Toshinori Tsuru
Pages 700-711

[Download PDF](#) [Article preview](#) 

Research article [Full text access](#)

Advanced multi-nozzle electrospun functionalized titanium dioxide/polyvinylidene fluoride-co-hexafluoropropylene (TiO₂/PVDF-HFP) composite membranes for direct contact membrane distillation

Eui-Jong Lee, Alicia Kyoungjin An, Pejman Hadi, Sangho Lee, ... Ho Kyong Shon
Pages 712-720

[Download PDF](#) [Article preview](#) 

Research article [Full text access](#)

The mechanical strength of a ceramic porous hollow fiber

Patrick de Wit, Frederique S. van Daalen, Nieck E. Benes
Pages 721-728

FEEDBACK 

[Download PDF](#) [Article preview](#) 

Research article [Full text access](#)

UV-cured polysulfone-based membranes: Effect of co-solvent addition and evaporation process on membrane morphology and SRNF performance

Veysi Altun, Jean-Christophe Remigy, Ivo F.J. Vankelecom
Pages 729-737

[Download PDF](#) [Article preview](#) 

Research article [Full text access](#)

Effect of pore size on the interfacial resistance of a porous membrane

K.S. Glavatskiy, Suresh K. Bhatia
Pages 738-745

[Download PDF](#) [Article preview](#) 

Research article [Full text access](#)

Mixed gas sorption in glassy polymeric membranes. III. CO₂/CH₄ mixtures in a polymer of intrinsic microporosity (PIM-1): Effect of temperature

Aweke Elias Gameda, Maria Grazia De Angelis, Naiying Du, Nanwen Li, ... Giulio C. Sarti
Pages 746-757

[Download PDF](#) [Article preview](#) 

Research article [Full text access](#)

Comparative analysis of full-scale membrane distillation contactors - methods and modules

D. Winter, J. Koschikowski, F. Gross, D. Maucher, ... A. Hagedorn
Pages 758-771

[Download PDF](#) [Article preview](#) 

[< Previous vol/issue](#)

[Next vol/issue >](#)




Copyright © 2022 Elsevier B.V. or its licensors or contributors.
ScienceDirect® is a registered trademark of Elsevier B.V.



FEEDBACK 

Ads by Google

[Stop seeing this ad](#) | [Why this ad?](#)
also developed by scimago:  SCIMAGO INSTITUTIONS RANKINGS

SJR

Scimago Journal & Country Rank

[Home](#) | [Journal Rankings](#) | [Country Rankings](#) | [Viz Tools](#) | [Help](#) | [About Us](#)

Ads by Google

[Stop seeing this ad](#) | [Why this ad?](#)

Journal of Membrane Science

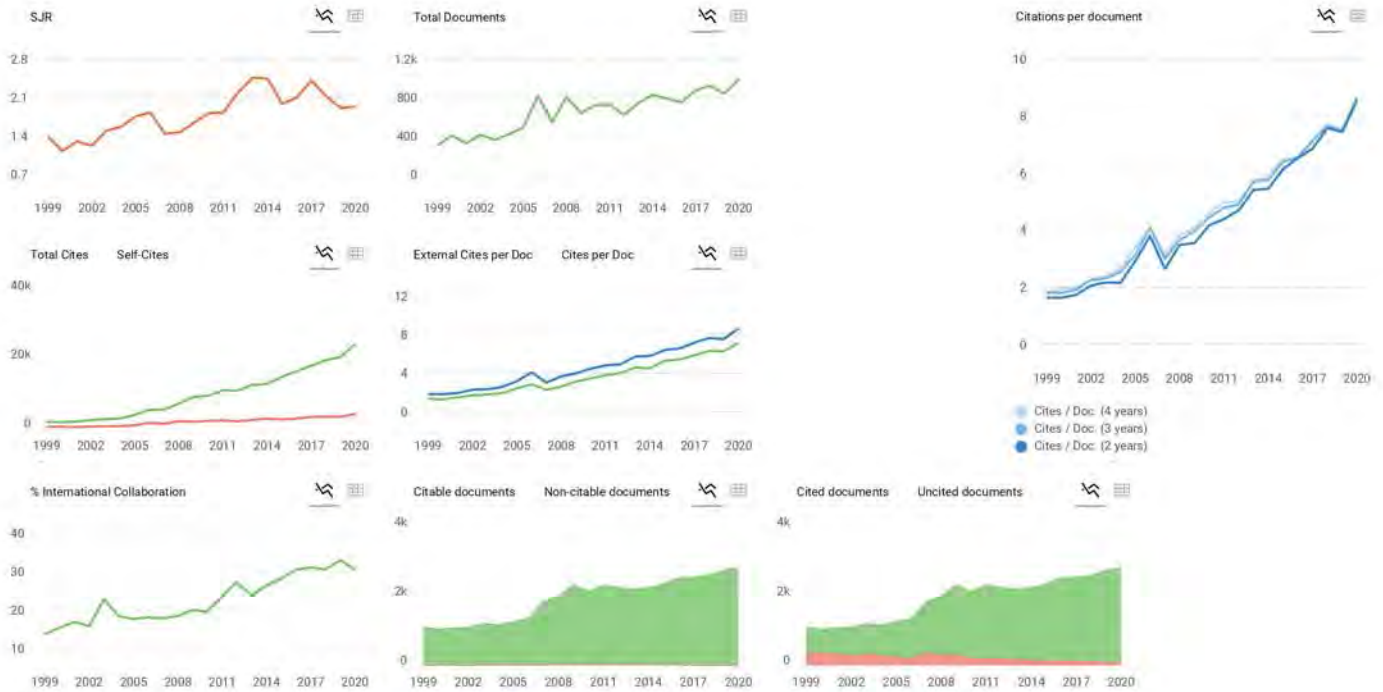
COUNTRY	SUBJECT AREA AND CATEGORY	PUBLISHER	H-INDEX
Netherlands Universities and research institutions in Netherlands	Biochemistry, Genetics and Molecular Biology Biochemistry Chemical Engineering Filtration and Separation Chemistry Physical and Theoretical Chemistry Materials Science Materials Science (miscellaneous)	Elsevier	249
PUBLICATION TYPE	ISSN	COVERAGE	INFORMATION
Journals	03767388	1976-2021	Homepage How to publish in this journal Contact

SCOPE

The Journal of Membrane Science provides a focal point for academic and industrial chemists, chemical engineers, materials scientists, and membranologists working on membrane systems. The journal publishes original research and reviews on membrane transport, membrane formation / structure, fouling, module / process design, and processes / applications. Primary emphasis is on structure, function, and performance of non-biological membranes; papers bridging the gap with biological membranes are also appropriate. The Journal of Membrane Science publishes Full Text Papers, State-of-the-Art Reviews, Letters to the Editor, and Perspectives. Reviews: should not only summarize the key research contributions in a field, they should also provide critical evaluation of the scientific literature. Review papers are intended to provide archival guidance and direction for the broad membrane community and are thus held to the highest standard for publication. Perspective articles: should provide a focused discussion of an important area of membrane science and technology, emphasizing recent developments, future challenges, and/or new opportunities. Perspective articles will be by invitation only, and they will be reviewed by at least one Editor of the Journal and one member of our Advisory or Editorial Board.

 Join the conversation about this journal

 Quantiles



Journal of Membrane Science

Q1 Biochemistry

sjr 2020 1.93

powered by scimagojr.com

Show this widget in your own website

Just copy the code below and paste within your html code:

```
<a href="https://www.scimagojr.com" >
```

SCImago Graphica

Explore, visually communicate and make sense of data with our new free tool.

Get it

Metrics based on Scopus® data as of April 2021

S Shabdiki 2 years ago

Can you help me know what is the ISI rank of Journak of membrane science?

reply

Melanie Ortiz 2 years ago

Dear Shabdiki, SCImago Journal and Country Rank uses Scopus data, our impact indicator is the SJR. Check our web to locate the journal. We suggest you to consult the Journal Citation Report for other indicators (like Impact Factor) with a Web of Science data source. Best Regards, SCImago Team

Leave a comment

Name

Email
(will not be published)



I'm not a robot reCAPTCHA
Privacy - Terms

Submit

The users of Scimago Journal & Country Rank have the possibility to dialogue through comments linked to a specific journal. The purpose is to have a forum in which general doubts about the processes of publication in the journal, experiences and other issues derived from the publication of papers are resolved. For topics on particular articles, maintain the dialogue through the usual channels with your editor.



Ads by Google

Stop seeing this ad Why this ad? ⓘ



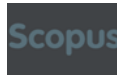
Ads by Google

Stop seeing this ad Why this ad? ⓘ

Developed by:

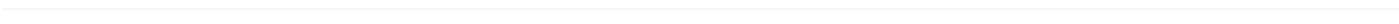
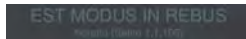


Powered by:



Follow us on @ScimagoJR

Scimago Lab, Copyright 2007-2020. Data Source: Scopus®





Source details

Journal of Membrane Science

Scopus coverage years: from 1976 to Present

Publisher: Elsevier

ISSN: 0376-7388

Subject area: Chemical Engineering: Filtration and Separation Chemistry: Physical and Theoretical Chemistry

Biochemistry, Genetics and Molecular Biology: Biochemistry Materials Science: General Materials Science

Source type: Journal

CiteScore 2020 ⓘ
13.5

SJR 2020 ⓘ
1.929

SNIP 2020 ⓘ
1.746

[View all documents >](#)

[Set document alert](#)

[Save to source list](#) [Source Homepage](#)

[CiteScore](#) [CiteScore rank & trend](#) [Scopus content coverage](#)

i Improved CiteScore methodology ×

CiteScore 2020 counts the citations received in 2017-2020 to articles, reviews, conference papers, book chapters and data papers published in 2017-2020, and divides this by the number of publications published in 2017-2020. [Learn more >](#)

CiteScore 2020 ▼

$$13.5 = \frac{48,502 \text{ Citations 2017 - 2020}}{3,604 \text{ Documents 2017 - 2020}}$$

Calculated on 05 May, 2021

CiteScoreTracker 2021 ⓘ

$$14.7 = \frac{54,922 \text{ Citations to date}}{3,745 \text{ Documents to date}}$$

Last updated on 06 March, 2022 • Updated monthly

CiteScore rank 2020 ⓘ

Category	Rank	Percentile
Chemical Engineering		
└ Filtration and Separation	#1/13	96th
Chemistry		
└ Physical and Theoretical Chemistry	#8/169	95th

[View CiteScore methodology >](#) [CiteScore FAQ >](#) [Add CiteScore to your site](#)

About Scopus

- [What is Scopus](#)
- [Content coverage](#)
- [Scopus blog](#)
- [Scopus API](#)
- [Privacy matters](#)

Language

- [日本語に切り替える](#)
- [切换到简体中文](#)
- [切换到繁體中文](#)
- [Русский язык](#)

Customer Service

- [Help](#)
- [Tutorials](#)
- [Contact us](#)

ELSEVIER

[Terms and conditions](#) ↗ [Privacy policy](#) ↗

Copyright © Elsevier B.V. ↗. All rights reserved. Scopus® is a registered trademark of Elsevier B.V.

We use cookies to help provide and enhance our service and tailor content. By continuing, you agree to the use of cookies.

